Molecular Dynamics Simulation of Clay Swelling during Low Salinity Waterflooding in Clay Rich Sandstone Reservoirs

by

Medet Yerkin

2020

Thesis submitted to the School of Mining and Geosciences of Nazarbayev University in Partial Fulfillment of the Requirements for the Degree of
Master of Science in Petroleum Engineering

Nazarbayev University

April 2020

ACKNOWLEDGEMENTS

I would like to express my gratitude and sincere thanks to my thesis supervisor, Dr. Ali Shafiei, for providing me with valuable guidance and regular suggestions as throughout this journey, and also for the opportunity to work under his project holding a state grant and for keeping me motivated and occasionally pushing me beyond my limits. I also would like to thank my co-supervisor, Dr. Jalal Foroozesh of Universiti Teknologi PETRONAS in Malaysia, for the ideas and perceptions in relation to the research topic and recommendations on the selection of methodology for this thesis work. Special thanks to my co-supervisor, Dr. Yanwei Wang, for sharing his knowledge on the basic theory and methods of molecular dynamics simulations and for useful meetings and discussions.

This work was part of the Faculty Development Competitive Research Grants Program (FDCRGP) grant entitled: "LSWF: Experimental and Modeling Investigation of Low Salinity Water Flooding in some Oil fields of Republic of Kazakhstan – Improved Oil Recovery Implications." I wish to acknowledge the financial support I received from this grant.

I would like to acknowledge National Supercomputing Center in Shenzhen, China, for providing the computational resources and Materials Studio (version 7.0, module Forcite).

I am indebted to my lab mate Askhat Abdrakhmaov for accompanying the long way from searching for the right software to finishing the simulation runs and for his support and guidance throughout this thesis work.

ORIGINALITY STATEMENT

I, Medet Yerkin, hereby declare that this submission is my own work and to the best of my knowledge it contains no materials previously published or written by another person, or substantial proportions of material which have been accepted for the award of any other degree or diploma at Nazarbayev University or any other educational institution, except where due acknowledgement is made in the thesis.

Any contribution made to the research by others, with whom I have worked at NU or elsewhere is explicitly acknowledged in the thesis.

I also declare that the intellectual content of this thesis is the product of my own work, except to the extent that assistance from others in the project's design and conception or in style, presentation and linguistic expression is acknowledged.

Signed on 15.04.2020

_____

NOMENCLATURE

Acronyms and Abbreviations

CEC	Cation exchange capacity
COMPASS	Condensed-phase optimal molecular potential for atomistic simulation studies
DHNA	Decahydro-2-napthoic acid
DLVO	Derjaguin, Landau, Verwey, and Overbeek theory
EOR	Enhanced oil recovery
IOR	Incremental oil recovery
LSE	Low salinity effect
LSW	Low salinity water
LSWF	Low salinity water flooding
MDS	Molecular dynamics simulation
Na-MMT	Sodium montmorillonite
NPT	Constant number of molecules, pressure, and temperature
NVT	Constant number of molecules, volume, and temperature
RDF	Radial distribution function
SAC	Surface active compounds
SARA	Saturates, aromatics, resins, and asphaltenes
TOT	Tetrahedral, octahedral and tetrahedral

Symbols

E_{angle}	Angle potential, (cal/mol) or (J/mol)
E_{bond}	Bond potential, (cal/mol) or (J/mol)
E_{oop}	Out-of-plane angle potential, (cal/mol) or (J/mol)
$E_{torsion}$	Torsional potential, (cal/mol) or (J/mol)
E_{cross}	Cross coupling interaction potential, (cal/mol) or (J/mol)
E_{elec}	Electrostatic interaction, (cal/mol) or (J/mol)
E_l	van der Waals interactions, (kcal/mol) or (kJ/mol)
T	Temperature, (K)
P	Pressure, (bar)

Greek Letters

$V(r)$	Potential energy, (kcal/mol)
K	Spring constant
r_{eq}	Equilibrium distance between the atoms, (nm)
θ_{eq}	Equilibrium angle between the atoms, (degree)
n	Multiplicity of the function
ϕ	Dihedral angle, (degree)
γ	Phase shift
ξ	Out-of-plane angle, (degree)

Metric Conversion Factors

1 Å	=	10^{-10} m
1 cal	=	4.184 J
^{o}K	=	273.15 + ^{o}C
1 cal	=	4.184 J
1 ppm	=	1 mg/L

ABSTRACT

Oil production from mature hydrocarbon reservoirs using EOR techniques has become an essential part of the petroleum industry. One of such EOR methods consists of injection of brine with decreased salinity. The concept of low salinity waterflooding (LSWF) is to increase the oil recovery factor by changing the reservoir rock's affinity from oil-wet or mixed-wet towards a more favorable condition through flooding the reservoir with desalinated seawater. This is a promising EOR method because of its accessibility, high oil recovery, and low expenses. However, uncontrolled injection of LSW may lead to clay swelling effect in some clear bearing sandstone reservoirs and cause a reduction in oil recovery due to the entrapment of crude oil because of the permeability impairment and decrease in porosity. In this work, we used molecular dynamics simulation (MDS) which is a very convenient tool to model interactions between organic molecules and clay surface. The objective of this research works was to investigate the optimum saturation of injected low salinity water ions, from 10-25% of formation brine at different water contents. The next research objective was to predict clay swelling effect during LSWF and at the same time achieving detachment of crude oil to get satisfactory incremental oil recovery. Sodium montmorillonite (Na-MMT) clay was selected which can absorb crude oil due to the negative surface charge and it is the most swelling clay mineral. The interaction between the clay minerals with oil and brine at different salt concentrations have been modelled. We present the results as a function of interlayer density profiles, basal d-spacing, and hydration energetics. The results demonstrated the least interlayer space for the Na-montmorillonite with the 25% salinity of initial formation brine salinity and the further decrease in water salinity leaded to generation of diffuse ion swarm. Insufficient number of counter-ions in one layer than other layers typically triggers clay swelling effect because of the system that is trying to dilute the concentration and restore and achieve balance. Insights obtained from this fundamental scientific research can further our current understanding of some of the mechanisms proposed for wettability alteration and oil recovery by using LSWF in clay rich sandstone reservoirs.

Table of Contents

List of Figures

List of Tables

1. INTRODUCTION

Low salinity waterflooding (LSWF) as an EOR method which involves continuous injection of brine with decreased salinity into the reservoir has gained a lot of attention in the recent years from both the oil industry and the academia. This is mainly due to the promising results in both laboratory and filed scale and its potential in recovering additional oil during tertiary stage of production (Bassir et al., 2016). The concept of LSWF is to increase production by changing rock affinity towards the desired condition with flooding desalinated seawater into oil-wet or mixed-wet reservoir. Although, there are some requirements for LSW to work and get positive response, one of them is the initial condition of the oil and presence of a mixed-wet rock (Katende et al., 2019).

Presence of clay minerals in a reservoir can affect the performance of LSWF. In fact, uncontrolled injection of LSW may lead to clay swelling effect in some reservoirs and can cause a reduction in oil recovery due to the entrapment of crude oil because of the permeability impairment and decrease in porosity. Kakati et al. (2020) reported clay swelling during injection of low salinity water into a sand pack. More studies on LSWF in sandstone confirmed the effect of increase in the size of clay mineral is caused by the injection of low salinity brine; while, the injection of high salinity water resulted in shrinkage of the clay (Marhaendrajana et al., 2018; Yuan and Wood, 2018; Mahmud et al., 2019). A model proposed by Austad (2010) shows the significance of active clay minerals for low salinity effect. The structure of the most clay minerals found in reservoirs consists of tetrahedral and octahedral aluminum layers. The negative charge of clay surface was promoted by the charge imbalance of silica or aluminum layer and at the edge surfaces.

1.1 Statement of the problem

Increase in oil production using some EOR methods such as LSWF is substantial and worth spending money and effort. However, every EOR method has its own advantages and disadvantages. In the case of LSWF, a major problem in sandstone reservoirs arise from presence of a high clay content in the reservoir rock (Mahmud et al., 2019). Swelling clays are the most troublesome minerals which in contact with water their volume increases and as a result causes a decrease in porosity and permeability of the reservoir. The decrease in pore space causes entrapment of the oil and decrease in oil mobility. Such reduction in porosity and

permeability of the reservoir results in decrease in oil recovery. According to Bernard et al. (1967), the leading mechanism of LSWF leading to high oil recovery is the impairment of permeability. Although, the contradictory statement of Bernard et al. (1967) was then further investigated and elucidated in terms of determining the driving mechanism of LSWF in sandstones which are multi-component ion exchange, double layer expansion, and pH increase (Austad et al., 2010). Recent findings from field implementations of LSWF showed that the decrease in the planned incremental oil recovery maybe due to clay swelling effect in sandstone reservoirs (McGuire et al., 2005; Lager et al., 2008). Therefore, this research work is dedicated for better understanding the clay behavior under LSWF and to determine an optimum concentration of low salinity water so that it does not trigger clay swelling and yet alters the wettability of the reservoir rock towards more water wet and therefore improves the incremental oil recovery.

1.2 Relevance to the industry

The economy of Kazakhstan is highly dependent on oil and gas sector because when it comes to the oil reserves ranking all over the world, they are among the top 15 countries (BP Statistical review of world energy, 2018). According to the report for 2017 of the National Oil and Gas Ministry of Kazakhstan, 62% of the whole country is occupied with petroleum with overall 172 oil fields and 80 of which is currently under development. The majority of those oil fields are sandstone reservoirs with a clay content of up to 35% and requires further development in terms of oil recovery, also the world's 50% of conventional sandstone reservoirs contain clay minerals. Implication of LSW as a tertiary oil recovery method will decrease the overall project cost, more importantly, it can achieve high oil recovery in comparison with other chemical EOR methods (Bassir et al., 2016). Although it may cause several problems as discussed before, porosity reduction and permeability impairment which in case will trap crude oil leading to the decrease in oil production (Sharifipour et al., 2017). Therefore, knowing the critical saturation of ions in injection low salinity water would be a game-changing factor in oil recovery.

1.3 Research objectives

This study aims to predict the clay swelling effect in sandstone reservoirs which is very crucial in terms of understanding the mechanism of LSWF in clay rich sandstone reservoirs at molecular scale and also determining an optimum salinity for the injected water. The optimal condition for a successful LSWF in a sandstone reservoir with active clay minerals is how to

optimize the salinity of the injected water so that it is enough to trigger wettability alteration and at the same time prevent clay swelling and impairment of fluid flow in the reservoir. To address this issue, in this research work we aimed at:

1. Evaluating the role of clay minerals in sandstone reservoirs during the LSWF in clay bearing sandstones;

2. Investigating the role of ionic composition and salt concentration during LSWF in clay bearing sandstones;

3. Developing a mechanistic model of oil compounds and understanding the interaction between oil components such as carboxylic group acids with clay mineral during LSWF in clay bearing sandstones.

1.4 Research methodology

This thesis work is a computational (molecular dynamics) study to understand the science behind the phenomenon of low salinity waterflooding at molecular scale in clay rich sandstone reservoirs. Using classical atomistic molecular dynamics the models of clay mineral surfaces, low salinity water and oil molecules were built. Unit cell of montmorillonite was generated substituting Al atoms to Mg atoms of the octahedral layer; while, the tetrahedral layer had two isomorphic substitutions. The resulting unit cell had a net negative surface charge which was counterbalanced by intercalating Na^+ cations. The simulation consisted of several dynamic production runs with different run time and time step to reach the equilibration of the system and generate oil-wet clay. In the end, production with 10 ns simulation time was ran to detach oil by adding low salinity water with ions of Na^+, Cl^-. The graphs of one-dimensional density profile with basal d-spacing to describe different swelling states of the montmorillonite and hydration energy against number of water molecules were generated. Finally, the correlation corresponded to 2W hydrates and swelling state of the montmorillonite was provided. The unit cell of Wyoming type montmorillonite with certain stoichiometry was taken from American Mineralogist Database.

1.5 Thesis structure

This thesis work is organized into 6 chapters according to the aims provided above. A brief description of each chapter will be provided below. Chapter 1 contains a brief introduction,

problem statement, relevance to industry, research objectives, and research methodology of this research work. Chapter 2 which is the literature review, includes background on LSWF in sandstone reservoir more specifically the importance of presence of clay minerals, driving mechanism for wettability alteration, adsorption of crude oil onto clay mineral, and clay swelling effect during the hydration. The information about the project plan and schedule with risk assessment in described is Chapter 3. In Chapter 4, first the general molecular dynamics work principle is explained and then the research methodology leading to development of the clay model and simulation parameters used is described. Summing up with the visualization and analysis sections, Chapter 5 includes the results of the simulation illustrated in graphs followed by a discussion section. Lastly, the conclusions and some recommendations for future work are presented in Chapter 6.

2. LITERATURE REVIEW

The demand for the energy sector is growing every day and interest in renewable energy is substantial. Although there is no doubt that in near future energy consumption from petroleum and other liquids will still be substantial. According to International Energy Outlook 2019 provided by the U.S. Energy Information Administration (EIA), the increase in petroleum consumption as an energy source will be nearly 50% between 2018 and 2050 and most growth comes particularly from Asia (Figure 1).

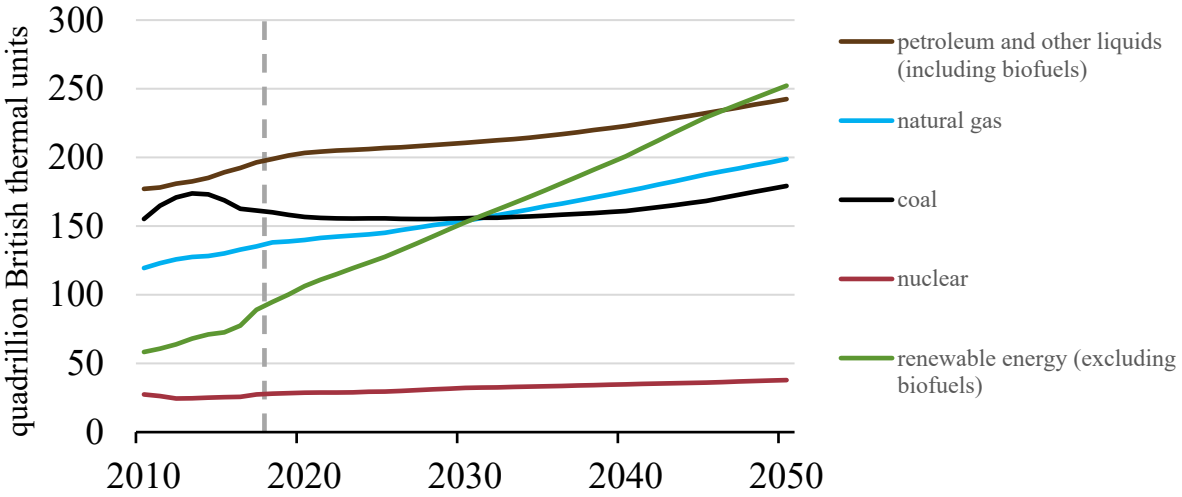

Figure 1. The global energy consumption from 2010 to 2050. Data have been extracted from the IEA International Energy Outlook 2019.

In the period of energy increase from sustainable energy due to the concerns on environmental impact caused by the combustible fuel. Even though it is demanded and will still be used as energy source for the future and relying on the annual international energy outlook report from 2019, the contribution of petroleum and other liquid-based fuels on total energy consumption will be nearly 73% (Figure 2). The forecast shows that the major consumer of petroleum fuel as an energy source will be the transportation sector. Thus, the petroleum energy sector is under challenge to maximize and optimize oil production from existing oil reservoirs.

After the drilling process is complete, the process of petroleum extraction (production) follows three steps, they are primary production (recovery), secondary recovery and tertiary (enhanced) recovery. The recovery factor from the primary flood on average varies between 5% and 35%. Although, it is highly dependent on the energy size of the reservoir.

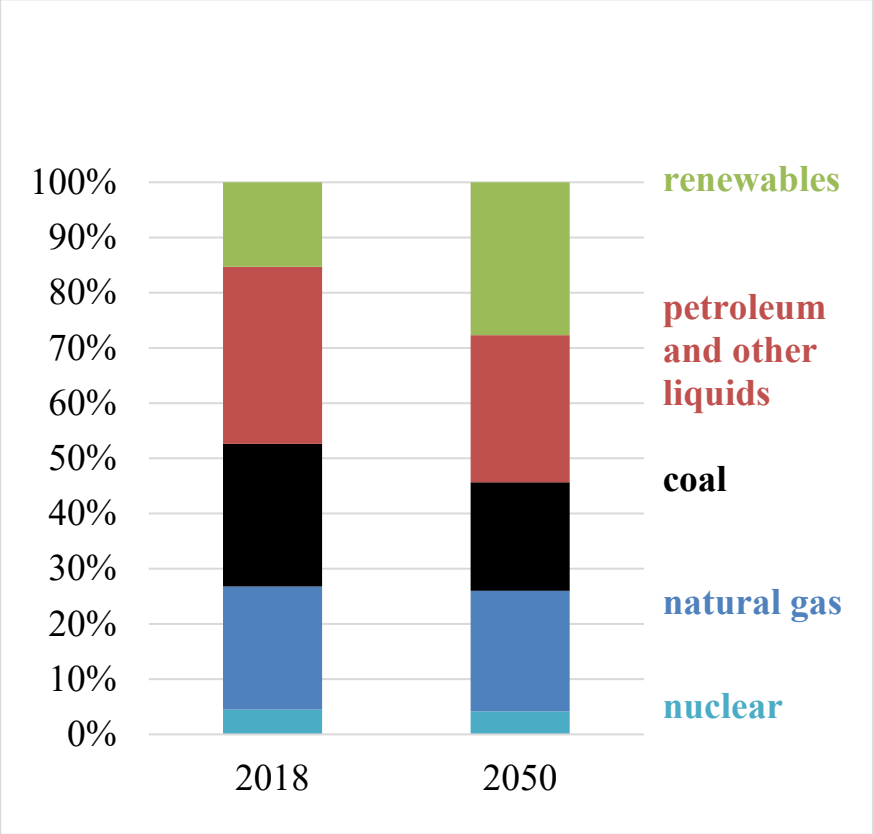

Figure 2. The global energy consumption from each energy source for 2010 and 2050. Data have been extracted from the IEA Internation Energy Outlook 2019.

The idea of secondary oil recovery is to inject external fluid or gas into the reservoir to displace hydrocarbon. The recovery from secondary flood method can be up to 30% in case of success. The main difference between secondary and enhanced (tertiary) recovery is that instead of just forcing fluid or gas into the reservoir, EOR changes rock and fluid properties to reach inaccessible oil (trapped in small pores) and achieve more incremental recovery. A successful implementation of enhanced oil recovery may be achieved up to 75%. The most common EOR methods are thermal methods such as steam injection; and chemical methods, such as mentioned before surfactant or polymer. One slowly grinding technique with appealing characteristics is low salinity waterflooding. This EOR method has been used in the industry for over than twenty years due to its advantages that other EOR techniques such as availability, comparatively low cost, environmentally friendly, and easy field implementation. Although, there is still no clear explanation on the working principle of it.

2.1 Low Salinity Water Flooding

The breakthrough finding on LSWF as an efficient oil recovery method was first found by Bernard et al. in 1958. Extraordinary findings of Bernard et al. stated that the recovery factor can be improved by using freshwater instead of high salinity water as an injection fluid specifically in sandstone reservoirs with high clay content. Moreover, in 1967 they found out the sweep efficiency is adjusted because of the mechanisms such as clay swelling and pore throat plugging from migration.

In-depth studies related to LSWF, that wettability will have modification towards water wetness were made in the 1990s by Jadhunandan and Yildiz, and Morrow. The effect of LSWF was tested by Webb et al. (2004), where they proposed “log-inject-log” test. The theory behind this test was that first by well logging techniques many parameters of core were measured, such as water saturation, oil saturation and temperature. Then low salinity water was injected, and they have finally logged again. The results were positive with an oil recovery improvement by 50%. It was also experimentally found that low salinity water flooding has a positive effect on the shape of the relative permeability curve and locations of endpoints, with high oil relative permeability at low water permeability (Webb et al., 2004; Kulkarni and Rao, 2005; Rivet, 2009; Fjelde et al., 2012).

LSWF was first applied to the Endicott oil field in Alaska by British Petroleum where 26% of incremental oil recovery (IOR) was achieved. In 2016 following the success of Endicott field, British Petroleum in partnership with ConocoPhillips, Chevron, and Shell have launched the biggest offshore low salinity waterflooding project, where calculations showed additional 40 million barrels of oil. Although the major mechanism behind low salinity water flooding is still a mystery, many big oil companies and studies have been conducting the laboratory and simulation tests to get the answer.

2.2 The Mechanism behind Wettability Alteration

The researchers have investigated that there are more than 17 mechanisms of low salinity water flooding leading to high IOR values and they are divided into two subclasses, they are either related to the fines migration or wettability alteration.

Tang and Morrow (1999) suggested that fines migration causes mobilization of residual oil, wettability alteration and flow path alteration is due to the fines detachment from the pore

surface after the contact with low salinity water in mixed or oil-wet system. This study influenced on sharp increase of interest in the identification of other mechanisms of low salinity water flooding. Like, McGuire et al. (2005) suggested pH increase at the effluent as a driving force from low salinity waterflooding, while couple of years later, the multivalent cations bounded to the polar oil components in the water film and water wetness achieved because of the oil detachment from the surface after ion exchange between low salinity water and water film was mentioned by Lager et al. (2006). Although, the detachment of organic material from the clay surface that changes wetness conditions is the primary cause for pH increase was reported by Austad et al. (2010) and put in doubt the finding of McGuire et al. The equation was proposed by Hamouda et al. (2014) on pH increase which is associated with fines migration in clay minerals causing an increase in pressure drop in the sandstone core sample. According to Ligthelm et al. (2009), the wettability modification in mixed and oil-wet sandstones can be relied on electrical double layer expansion due to the ionic strength reduction of brine film. Finally, Buckley and Morrow (2011) stated that the responsible one for the wettability alteration of low salinity effect (LSE) which caused mixed-wet fine particle release in kaolinite. Even though, they didn't exclude the effect of osmotic pressure which might also contribute to the rock wettability modification.

Supporting the idea of Lager et al. (2006), the further geochemical investigation was made by Pouryousefy et al. (2016) to understand the exact hypothesis behind multi-component ion exchange. Using the general concept of multi-component ion exchange which claims that because of the different attraction of cations towards the rock surface, the cation exchange process happens on the surface of the minerals. Substitution of divalent cations which monovalent cations occur when initial equilibrium state disturbed by the injection low salinity water due to the difference in ionic concentration with initial formation water.

Pouryousefy et al. (2016) in his experiment claims that ion exchange takes place in geochemical reaction, in aqueous and mineral dissolution, but it is worth mentioning that many studies that state the superiority of dissolution of surface did not take into consideration the zeta potential in the oil-water emulsion suspension while only focusing on brine suspensions. Aqueous reactions are the spontaneous ones, while mineral dissolution is represented as rate-dependent chemical equilibrium reaction. As a result of the experiment, they conclude that chemical bonds given in Figure 4 are highly affected by the electrolyte concentration of the injected water and formation water (Figure 3).

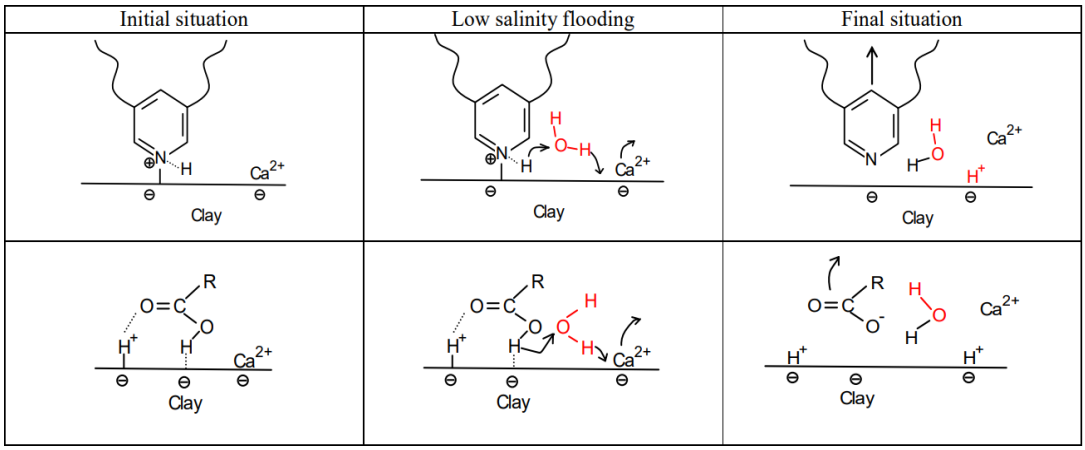

Figure 3. Austad proposed mechanism for low salinity EOR effects. Upper: Desorption of basic material. Lower: Desorption of acidic material. (retrieved from Austad et al., 2010)

In their simulated model, it claims that if multi-component ion exchange is the major mechanism of low salinity water flooding then recovery factor is expected to be lower because the role of cation exchange capacity in the experiment was negligible while it should affect significantly. Therefore, Pouryousefy et al. (2016) suggested that multi-component ion exchange is not the only mechanism of wettability alteration because it cannot break chemical bonds (Figure 4) without sufficient repulsive force. The repulsive force is explained as disjoining pressure that is a direct mechanism of electrical double layer expansion. By the given result, they put in doubt the dominant mechanism behind wettability alteration.

What is the exact mechanism behind wettability alteration? There are many suggestions for this question, but the most likely ones are only 4. They are multi-component ion exchange, double layer expansion, particle release and pH increase at the effluent. Although, a couple of studies proved that the last mechanism had some discrepancies due to the fact that in a real test results of pH value at the effluent of the core sample was fluctuating. Not only pH increase at

the effluent was contradicted but also particle release was also put in doubt claiming that it is the resulting effect caused by double-layer expansion rather than primary mechanism leading to wettability alteration.

Despite the fact that there is still no consensus on the driving mechanism of LSWF, recent findings observed required conditions for this EOR to work, such as rock characteristics, ionic composition of the low salinity water, and presence of organic components in crude oil.

2.2.1 The composition of injection and formation brine

The major parameter that affects the wettability alteration was considered to be the injected brine. When the talk is about the benefit of oil recovery from low LSWF we mean that the salinity of injected water should be lower than the connate water. Although, there were many misleading and overgeneralized concepts that the salinity water injected water did not play much of a role in achieving positive IOR. They are experimental studies of Sharma and Filoco (1998) where they investigated that the injected water did not affect oil recovery and claimed that the connate water composition plays much more important role; Zhang and Morrow (2006) where overall presented data showed that lower salinity water injection had relatively less oil recovery than higher salinity water injection. It was stated that manipulation of calcium, magnesium and sulfur ions could lead to the increase in IOR, also by the additional increase of sulfur ions lead to further increase in oil recovery up the residual oil saturation. However, Yildiz and Morrow (1996) did a very interesting experiment using two different scenarios (Brine 1 with 4%NaCl + 0.5% $CaCl_2$ while Brine 2 was 2% $CaCl_2$) with two different crude oils (Alaskan and Moutray). The results showed that when the injected brine and connate water salinity was the same, oil recovery was higher for 5.5% using Brine 2. The same procedure repeated but for different crude oil and in that case Brine 1 took advantage on Brine 2 with 16% lead of oil recovery. This interesting finding explains that the oil composition and ageing condition is very important in LSWF and will be discussed in next sub-section below.

Nonetheless, most of the experiments and pilot tests confirmed high oil recovery could be achieved when the salinity of injected water is lower than the interstitial water salinity. The sharp increase in oil recovery was mentioned by Zhang et al. (2007) when the injected water salinity was 1500 ppm or 5% of original formation water salinity and further slight increase can be attained when supplementary divalent ions such as SO_4^{2-} were added to the injection brine.

According to Jerauld et al. (2008), the results from the laboratory and the field suggested using salinity of injection brine 10-25% of connate water salinity or 1000-2000 ppm.

The requirements for the formation water also exist, like the presence of active cations such as Ca^{2+}. Austad et al. (2010) stated that the effect of low salinity water flooding is depending on cations initially absorbed onto the clay surface, also protons and organic materials. If the absorbed organic material is low in amount, where pH might be 6-7, also active ions absorption will increase the pH in low salinity water flooding due to the desorption and the effect of low salinity will be low, because the system is already water-wet. Consequence of having high active ion concentration above average is that it requires the management of initial pH for optimal absorption conditions.

2.2.2 Oil chemistry in LSWF

Significance of oil chemistry was mentioned by Mwangi et al. (2018) that it plays the same role on rock, brine and oil system as low salinity brine does, by generating required condition. The interaction between the mineral surface and oil, more specifically, organic compounds in oil is based on electrostatic forces or in other words, non-bonding interactions. The most common acid component inside cure oil is naphthenic acid, and it acts as an anchor between the mineral and crude oil for both sandstone and carbonate rock types (Standnes and Austad, 2003). It was using Berea sandstone (where 92% of the whole rock is quartz which is water-wet, and only 8% is either clay or other carbonate cements) with additives to the non-polar pure decane ranging between 100 and 4000 ppm of surface-active compounds (SAC). After conducting flotation qualitative method with initial water-wet systems, the highest adsorption or oil-wetness was achieved when the system had long-chain myristic acid at 4000 ppm. Although using the 2000 ppm of SAC showed promising results differing only for 8% than in the case of 4000 ppm. The oil-wetness generated by long-chain naphthenic acid was also worth mentioning. Author explains this phenomenon with the presence of clay minerals in sandstone where the majority reactive surface area of clay is seen by oil due to its small grain size, high surface area and the negative surface charge. Even though the negative surface charge of the clays is balanced with counter-ions such as sodium, calcite or caesium, it also attracted by the positively charged bases and carboxyl groups present in the oil-water interface. Thus, the oil adhesion towards the clay surface is controlled by the electrostatic interactions between the negatively charged surface and positively charged oil surface active components (Brady and

Krumhansl, 2013). Higher the numbers of SACs, such as bases and carboxylic groups in crude oil, higher the chances of making surface more oil-wet (AlOtaibi et al., 2011).

Another study was conducted on aqueous crude oil adsorption onto the clay mineral. The characterization of each complex components in crude oil is almost not possible claimed by Greathouse et al. (2017). Thus, analysis of crude oil with separate hydrocarbon group type is the commonly used one. One of this kind of analysis based on the polarities and solubilities of the compounds is called "SARA" which defines four fractions such as saturates (S), aromatics (A), resins (R), and asphaltenes (A) (Speight et al., 2007). The most relevant of them to multicomponent ion-exchange mechanism are polar components, the resins and the asphaltenes. The resin model used in this study was Decahydro-2-napthoic acid (DHNA) (Aitken et al., 2004) which is the most abundant in the petroleum reservoirs in deprotonated anionic form (Lee et al., 2010). Although, in this study, both protonated and deprotonated form has been used. Using the classical atomistic MD simulations the results showed positive result of protonated and deprotonated DHNA on adsorption to the negatively charged montmorillonite surface, also the adsorption did not depend on overall salinity of the system.

Not only polar acidic components are the primary agents in crude oil that create desired initial system for LSE, but the presence of basic properties in a hydrocarbon is also responsible for generating the suitable condition for the absorption onto reservoir minerals. Harve et al. (2003) stated that the relative absorption activity is dependent on the pH number and depending on the conditions both anionic and neutral form of the acid can absorb onto reservoir minerals.

Lager et al. (2008) reported four adhesion mechanisms of polar ends of crude oil on the clay surface. They are Van der Waals, cation exchange, ligand bonds and cation bridging (Figure 4).

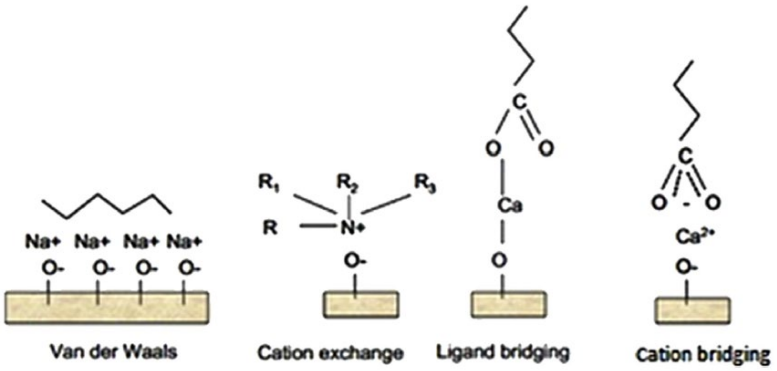

Figure 4. Representation of the diverse adhesion mechanism occurring between clay surface and crude oil (retrieved from Lager et al., 2008a)

It was also mentioned that the strongest bonds that can lead to the detachment of organometallic complexes are Van der Waals, cation exchange and ligand bonds.

2.2.3 The presence of clay mineral in a sandstone reservoir

Despite the necessity of controlling the parameters of injected low salinity water and oil composition, it is also critical to estimate reservoir characteristics. It has been pointing out the eminence of clay minerals on low salinity water flooding in sandstone rocks due to its effect on the wettability state of rock. The question arises from what type of clay mineral should be used to get maximum positive response? There are different types of clays, such as pure and mixed layer clays and each of those minerals has its own unique characteristics. For example, pure clays which are composed of kaolinites are believed to be an oil-wet system while smectite or chlorite are water-wet. Although, it is clear that the presence of polar components in crude oil may generate an oil-wet system in such clays as smectite and chlorite. Despite a lack of pure clays present in geological formations there have been conducted many studies on pure clays. Although, it has been proved that the occurrence of mixed-layer clays are more likely in geological formations. The attention should be given to that montmorillonites are most likely to occur in those mixed-layer clays. During the process of low salinity water injection is was stated that the clay's electrical double layer expands (DLVO theory). As we know clay surface is negatively charged which means any positively charged molecule will bond to the surface or to the Stern layer of the surface while negatively charged molecules will get repelled. After further attraction of charged molecules, electrical double layer of clay is tended to expand (increase in diffuse layer) and starts to interact with surrounding molecules which in case may lead to the bulk swelling (Figure 5). This process might cause fines release and migration with oil molecules attached to the surface (Figure 6). Those mentioned two mechanisms are also types of wettability alteration mechanisms alongside with multicomponent ion exchange.

The reason behind the selection of montmorillonite among other clay minerals is that the montmorillonite is tended to be the most swelling, which is directly related to the hydration energy of the Na^+ leading to the greater swelling values than any other clay model. Question arising here is why only montmorillonite, why can't we use kaolinite and other clay group minerals? We can use kaolinites to achieve wettability modification but it is not our research interest because according to Tang and Morrow the kaolinites are more likely to detach from the surface rather than swell. The negative surface charge of montmorillonites is due to the substitutions of ions in the layers, such as Si by Al in two tetrahedral layers and Al by Mg in an octahedral layer.

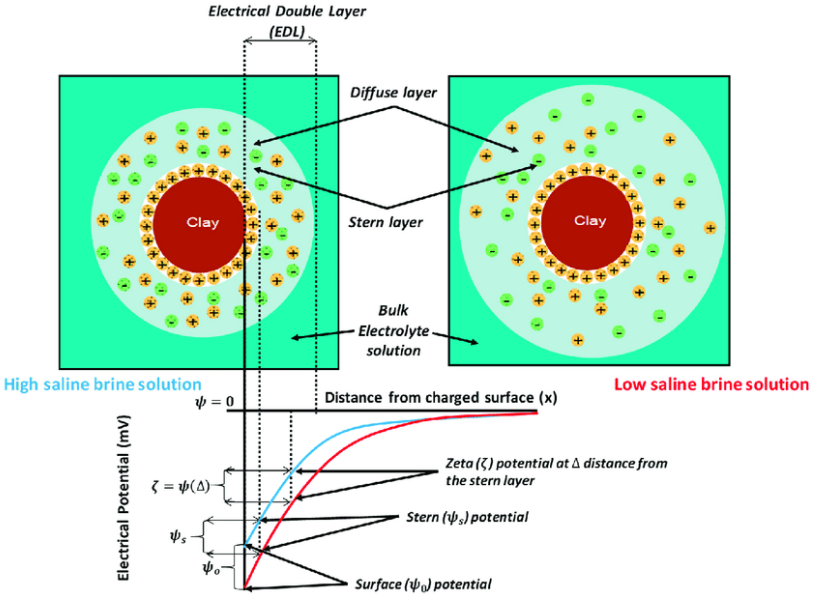

Figure 6. Illustration of the electrical double layer expansion in sandstone reservoirs (retrieved from Awolayo et al., 2018)

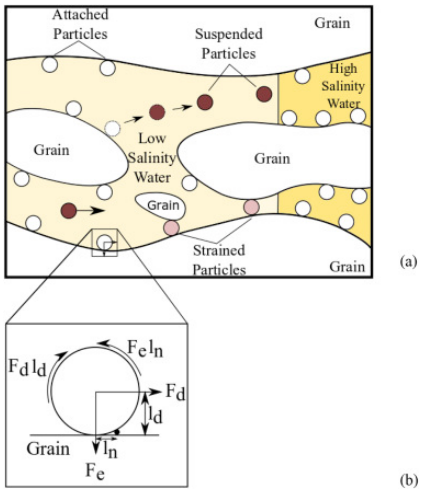

Figure 5. Schematic illustration of fines migration (a) attached, suspended, and strained particles during low-salinity water injection; (b) torque balance for electrostatic and drag forces on an attached particle (retrieved from Yang et al., 2019)

According to Sposito's "The Chemistry of Soils" there are eight different mechanisms that can describe the oil attraction to a clay surface. Although, Lager et al. (2008) stated that only four of those are potentially the right mechanisms for low salinity water flooding. They are cation exchange, cation bridging, ligand exchange and water bridging. In addition, pH effect was discussed where it could act as an alkaline flood in presence of low salinity water but the recent studies eased the hypothesis of akin acting low salinity water.

In order to have a positive response from low salinity water flooding, it is necessary to have clay mineral on initial formation water, especially Ca^{2+} to observe low salinity water flooding effects. Clays are characterized as a cation exchange mineral due to the structural charge imbalance, and tetrahedral silica and octahedral aluminium layers causing a negative charge on the clay surface. Kleven and Alstad (1996) suggested that the relative replacing the power of cations as follows:

$$Li^+ < Na^+ < K^+ < Mg^{2+} < Ca^{2+} < H^+ \quad (1)$$

It is worth mentioning that H^+ has the strongest affinity towards the clay surface at a certain concentration, but it many cases concentration of H^+ is less than the concentration of the formation water at pH = 4-5. Obviously, at equal concentrations, Ca^{2+} can displace more Na^{2+}.

2.3 Understanding Clay swelling effect

The swelling property of the clay mineral, more specifically montmorillonite of smectite group is an inescapable phenomenon in many industries. This is due to the complexity of being able to determine the interactions of water molecules with exchangeable cations or with the montmorillonite layer. As it was mentioned before for the successful implication of low salinity waterflooding in sandstone reservoir the presence of clay minerals plays a significant role. According to Kakati et al. (2020), the swelling of the clay happened during the injection of low salinity water into the sand packs. More studies on LSWF in sandstone confirmed the effect of increase in the size of clay mineral is caused by the injection of low salinity brine, while the injection of high salinity water resulted in shrinkage of the clay.

The abundance of smectite clays are dependent on the weathering conditions and tent to be the resulting product of the decomposition of igneous rocks. They are mostly formed in two tetrahedral layers made of silica sheets and one octahedral layer from aluminium sheets in between (T-O-T) and isomorphic substitutions may occur either in a tetrahedral or in an

octahedral layer. The clay minerals (platelets) were controlled by the interaction of negatively charged layer and positively charged interlayer cations or in other word counter-ions. Also, those interlayer cations can easily absorb water and further swell due to the limited layer charge (Figure 7). There are many factors affecting clay swelling such as temperature, pressure, humidity and composition of the solution.

The distance between the layers (TOT) is variable and addition of the thickness of one layer represents the basal d-spacing of the montmorillonite. There are two types of swelling with two different ranges of basal d-spacing. They are crystalline swelling where the increase in distance for the dehydrated state starting from ~10 Å (1 Å = 0.1 nm) reaches up to ~19 Å, while for the second type of swelling which osmotic swelling the layer spacing may vary between ~40 Å and onwards. In the oil and gas industry the most appealing scenario of production of crude oil it from the big pores, rather than from the small pores where the hydrocarbon is trapped. The osmotic swelling of clay mineral is caused by the cation exchange

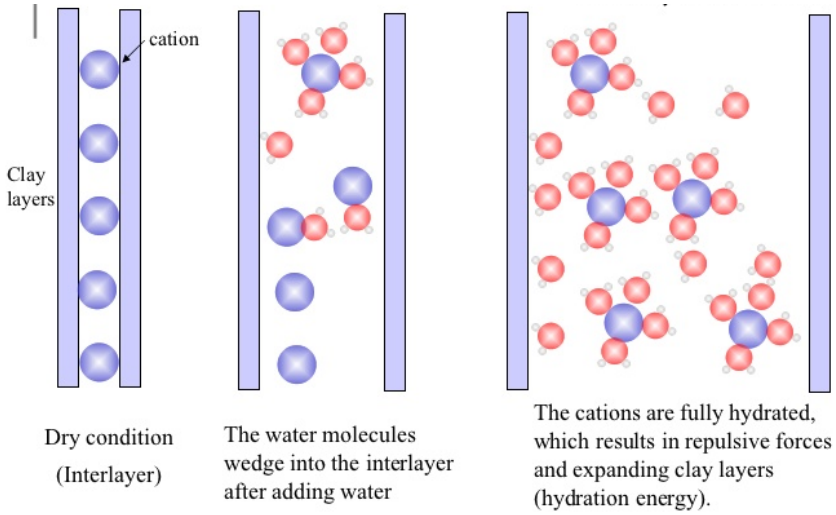

Figure 7. Courtesy of "An Introduction to Geochemical Engineering" Robert D. Holtz

between the TOT layers. When the cation concentration of one interlayer increases and becomes more than the relatively nearby interlayer, water tries to invade the area of lower cation concentration interlayer to dilute the concentration to restore and achieve balance. Further, this leads to the distance between the layers and triggers the clay swelling effect. During the injection of LSW, there will be the exact same phenomenon due to the additional cations of Na^+ present in the LSW. Therefore, in this study, we will study the phenomenon of crystalline swelling.

According to the report from Liu et al. the general trend of increasing basal d-spacing was related to the large charge location. In the case of Liu et al. basal d-spacing increased as a large charged shifted from the octahedral to the tetrahedral layer. Chavez-Paez et al. stated that this effect was more relatable for a Wyoming montmorillonite where a quarter of the layer charged shifted from octahedral to the tetrahedral layer. The increase in clay size which is the direct indication of the increase of basal d-spacing is the aftereffect of the charge increase on the tetrahedral layer for Na-Montmorillonite (Skipper, Sposito, & Chang, 1995). Also, the author indicates that in montmorillonite weaker ion-surface interactions result in the formation of fully hydrated ions (two-layer hydrate) at much lower water contents which in case leads to the swelling.

The problem arising here is that the osmotic swelling during the laboratory experiments has not found and called were forbidden basal spacing. Nevertheless, the study conducted by Fink and Thomas confirmed the existence of osmotic swelling and claimed several factors may be the responsible for such phenomenon, even though the explanation was not given due to the lack of information under the direct laboratory investigation. Although, using molecular dynamics simulations inconsistency of Na-montmorillonite structure may be the proper alternative to gather the required information.

2.4 Molecular Dynamics Investigation on LSW Mechanisms

The usage of a laboratory to face the objectives of this study is very hard. It may take too much time to predict clay swelling effect using certain concentrations and to find supercritical saturation of injection fluid it also required a lot of very expensive resources. Therefore, there is molecular dynamics simulation (MDS) that solves the problem of re-conducting the same experiment over and over again. The MDS has become an essential adjustment of laboratory experimental methods.

The general idea of molecular dynamics simulation is described as movement of atoms and molecules. They are allowed to interact at the fixed time and the trajectories were determined by the Newton's equation of motion where the force is described as a potential energy between the particles:

$$F = -\frac{d}{dr}V(r) \text{ or } F = -\nabla V \qquad (2)$$

V(r) is the force field and define the energy between the atom, such as bonds between the atoms; angles between the three atoms; dihedrals between the four atoms and rotation of the bond between the central bond; improper is the angle between the planes of four atoms (Figure 8).

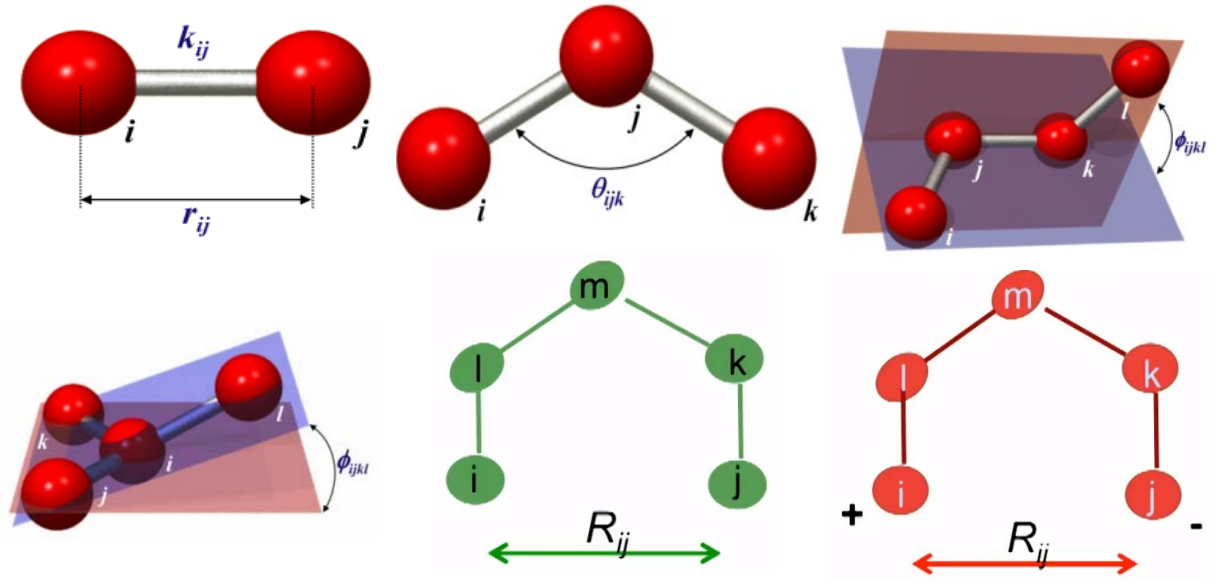

Figure 8. Force fields. Potential energy between the atoms. From top left to the bottom right: harmonic bonds, harmonic angle, dihedral angle, improper and nonbonding interactions (Van der Waals and electrostatic).

$$V(r) = \sum_{bonds} K_r(r - r_{eq})^2 + \sum_{angles} K_\theta(\theta - \theta_{eq})^2 + \sum_{dihedrals} \frac{V_n}{2}[1 + \cos(n\varphi - \gamma)] + \sum_{improper} K_\xi(\xi - \xi_0)^2 + \sum_{i<j} \left[\frac{A_{ij}}{R_{ij}^{12}} - \frac{B_{ij}}{R_{ij}^{12}}\right] + \sum_{i<j} \frac{q_i q_j}{\in R_{ij}} \quad (3)$$

The molecular dynamics study conducted by Underwood et al. (2017) to understand the clay surface during the injection of brine with varying salinity once again confirms that the organic compounds in crude oil are the primary factors for generating desired conditions. The organic molecules used for this study were protonated polar neutral decanoic acid and charged sodium decanoate. According to Underwood et al. each of those components were ideally suitable for different bridging mechanism due to the acid pH difference acid dissociation constant (pKa) (Barratt et al., 1996). For instance, using polar decanoic acid was perfect to

represent cation-polar bridging and deprotonated decanoate acid was good to probe cation-charged bridging effect. The simulation results for initial oil-wet sodium montmorillonite illustrated that the deprotonated decanoate acid has no contribution to the wettability of a clay surface. In the case of protonated polar decanoic acid desorption of non-polar decane from the clay surface was highly dependent on the salinity of the brine and replacing divalent ions in the system with monovalent ions increased the recovery factor.

In the work of Underwood et al. (2015) claimed that the mechanism representing the oil-cation-clay bridging between divalent ions of calcium and unchanged polar molecule is cation-polar exchange (Figure 9). Using the previous knowledge on acids present in crude oil the best fitting mechanism would be cation-charged bridging which is the bridging between calcium ion and charged deprotonated acid.

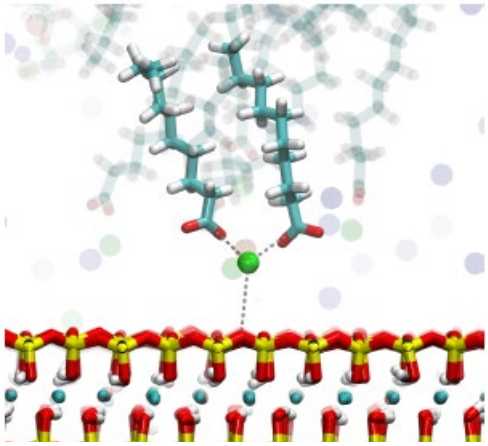

Figure 9. Charged cation bridging mechanism between the Na-MMT and charged sodium decanoate acid (retrieved from Underwood et al.)

The extended investigation on initially oil-wet Na-montmorillonite showed that the presence of any non-polar decane with other polar protonated and deprotonated decanoic acid did not give the required effect, they formed aggregates after setting up the simulation with water at different salt concentration. Although, the author mentioned the role and the effect of divalent cations such as Na^{+} and Ca^{2+} present in oil chemistry where the clay surface maintained oil-wetness despite the effect of salt concentration. Therefore, the pH level surrounding the clay surface and the protonation of the acids inside the crude oil plays a significant role and can be used for the appealing recovery factor from LSW.

3. PROJECT PLAN

3.1 Project schedule

The work can be well-completed on time with assigning due date of each part and planning is essential in this kind of projects. The essential tool provided by Gantt chart is the exactly go-to tool to meet the deadline and finish the job properly and in a well-organized manner. This thesis work's milestone has been provided in a Figure 10.

Tasks/Time	May				September				October				November				December				January				February				March				April			
	1	2	3	4	1	2	3	4	1	2	3	4	1	2	3	4	1	2	3	4	1	2	3	4	1	2	3	4	1	2	3	4	1	2	3	4
Introduction								x																												
Literature Review																																				
Final submission of Literature Review				x																																
Development of Methodology								x																												
Learning GROMACS				x																																
Learning LAMMPS and VMD								x																												
Running Sample Simulations												x																								
Learning Material Studio																		x																		
Generating clay model (NaMMT)																					x															
Calculating LSW ion concentration																						x														
Generating Crude Oil Layer																							x													
Running Simulations																														x						
Results and Analysis																															x					
Conclusion and Recommendations																																x				
Preparation for the Thesis Final Submission																																	x			
Final Thesis Submission																																		x		
Thesis Defence Preparation																																				x
Dissertation Defence																																				x

Figure 10. Gantt chart of thesis project plan

x – milestones

The sequence of plans is selected in order to meet the requirements on time management. After the topic of this thesis work was selected the objectives and thesis research questions were raised. In order to answer those questions literature review has been done and selecting the methodology the data collection has been conducted. At the beginning the selection of methodology lead to some problems due to the lack information and knowledge on that sphere. Nevertheless, after the investigation the proper software has been selected and simulation of initial system with varying parameters have started. The end of this project was finished with the analysis and suggested recommendations on future work for this thesis.

3.2 Resource requirements

The required software with the help of Dr. Yanwei Wang was delivered by the collaboration with National Supercomputing Center of Shenzhen (Shenzhen Cloud Computing Center). The manuals, sample simulation, and computers for performing the simulations were also provided.

All of the data are provided by the open database. Following Table 1 shows the selected equipment required for this thesis project.

Table 1. Required resources

Device/material	Function
Laptop or PC	My own laptop or PC from the computer laboratory is used to conduct the research
Access to internet	To download materials related to my thesis
Materials Studio by Accelrys	To build the system, run simulation and to collect the result.

3.3 Risk management

Table 2. Risk ranking matrix

Risk matrix		Consequence				
		Negligible	Minor	Moderate	Major	Catastrophic
Likelihood		1	2	3	4	5
Almost certain	5	6	7	8	9	10
Likely	4	5	6	7	8	9
Possible	3	4	5	6	7	8
Unlikely	2	3	4	5	6	7
Very unlikely	1	2	3	4	5	6

Risk rating	
Extreme	≥ 8
High	7
Medium	5-6
Low	≤ 4

Risk is a measure of probability of not achieving expected outcome, and it can be avoided or mitigated through well thought out planning. Risk mitigation plan was developed for this thesis to identify the possible risks and the ways of avoiding or controlling them. One of the common risk assessment tool is WRAC analysis that uses a 5x5 likelihood-consequence matrix. Table 2 illustrates the risk rating from low to extreme cases.

3.3.1 Physical hazards

Physical hazard is a factor that can harm a person's mental or physical condition without the need for physical contact. The possible physical hazards that can occur during the thesis work and the ways to avoiding them are given in Table 3.

Table 3. Physical hazards

Physical Hazard	Description	Risk rating	Risk Control
Eye-strain	Fatigue of the eyes due to prolonged presence in front of the computer screen	7 High	Regular exercise for eyes, regular breaks during using the computer
Injury during a workout at the gym	Mangle from lifting heavy weights	7 High	Heavy weight lifting under supervision, suspension belt use
High stress	Irritation from the overwork	5 Medium	Good study/relax balance, proper time management
Illness	Disease from mild colds to flu	3 Low	Maintain immunity of the body, dress warmly at cold conditions, stay away from sick people

3.3.2 Project hazards

Project hazards are the factors that can affect to the provision of the thesis on time due to unexpected situations.

Table 4. Project hazards

Project hazard	Description	Risk level / rating	Risk control
Sudden computer crash	Accidental fall to the floor	2 Low	Obligatory carrying in a bag
Thesis related documents loss	Sudden failure of the hard drive, computer crash due to viruses, not saving the thesis files	5 Medium	Use cloud services like google drive, do not forget to save, installation of anti-virus software
Change of thesis supervisor	Supervisor may be unable to continue student supervision due to some circumstances	5 Medium	Advice with co-supervisor or another professor competent in student's thesis topic
Software inaccessibility	Access to Materials Studio software	3 Low	Contact support team

4. METHODOLOGY

The methodology part of the research contains information on model construction starting with the generation of a unit cell according to pre-existing crystallography databases, layer properties of formation brine, and LSW layers with varying salt concentration. The generation of hydrocarbon layer with the organic compound has been modelled to achieve oil-wet condition. Then, the selection force field for the research has been explained and interaction energy for the COMPASS force field was introduced. A step-wise procedure of the simulation work is illustrated in the diagram with details on simulation parameters such as ensemble selection, buffer width, and cutoff distance are described. Finally, the visualization section was provided to explain the color scheme of all the illustrated figure below.

4.1 Model Construction

The Na-montmorillonite is the member of smectite group which is very soft phyllosilicate mineral as known as clay. The clay model used in this study was Wyoming-type montmorillonite with a unit cell dimensions of $5.16 \times 8.966 \times 9.347$ Å^3 and octahedral layer of the clay contained one Mg atom for every eight Al atoms. According to Ngouana et al., (2014) the most statistically accurate clay model was used and the resulting unit cell had a single negative charge and counterbalanced with Na^+ cations in the simulation of Na-montmorillonite (Figure 11). Therefore, the original crystal structure of montmorillonite unit cell was referred to Nhouana et al. The electric charges of the atoms and their location coordinates were assigned by the CLAYFF force field and the final unit cell generated net negative surface charge of -0.75e. Although, in this study COMPASS force field was selected to represent clay mineral even though, the net charge of the unit cell will remain the same.

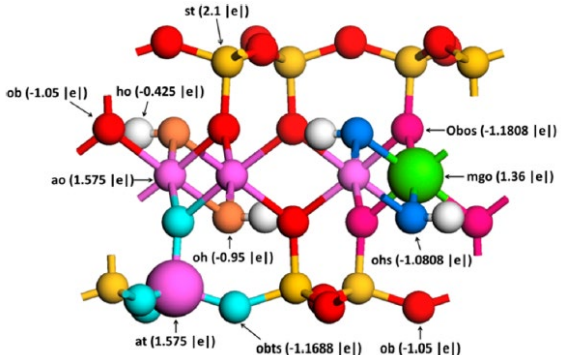

Figure 11. Montmorillonite unit cell in this study. Ob (bridging oxygen), Obts (bridging oxygen with tetrahedral substitution), Obos (bridging oxygen with octahedral substitution), Oh (hydroxyl oxygen), Ohs (hydroxyl oxygen with octahedral substitution), at (Al in tetrahedral sheet), ao (Al in octahedral sheet), mgo (Mg in octahedral sheet) and st (Si in tetrahedral sheet) (retrieved from Ngouana et al., 2014).

The basal {001} surface of montmorillonite has a relatively stable pH value and may be the good representation of the real oil reservoir. Then for the case clay swelling effect prediction supercell of $4 \times 4 \times 3$ was created along a, b and c crystallographic directions with overall 48 cells. The overall system with keeping Mg/Al in the octahedral substitution on the same position while Si/Al substitution on the tetrahedral sheet was randomly positioned after which they were assigned to obey the Loewenstein's rule with proportions for each TOT layer of 4 Al per 124 Si and 8 Mg per 56 Al. This was managed to obtain general unit cell of Wyoming-type montmorillonite with a chemical composition of $Na_{0.75}(Si_{7.75}Al_{0.25})(Al_{3.5}Mg_{0.5})O_{20}(OH)_4$. Final clay model represented a degree between the pairs of lattice vectors $\alpha = 90°, \beta = 90°, \gamma = 90°$, and the system size of $a = 20.6768$ Å, $b = 35.8245$ Å, $c = 51.6859$ Å. The overall system consisted of three TOT layers with intercalated formation water, hydrocarbon and LSW one of those systems was demonstrated in Figure 12.

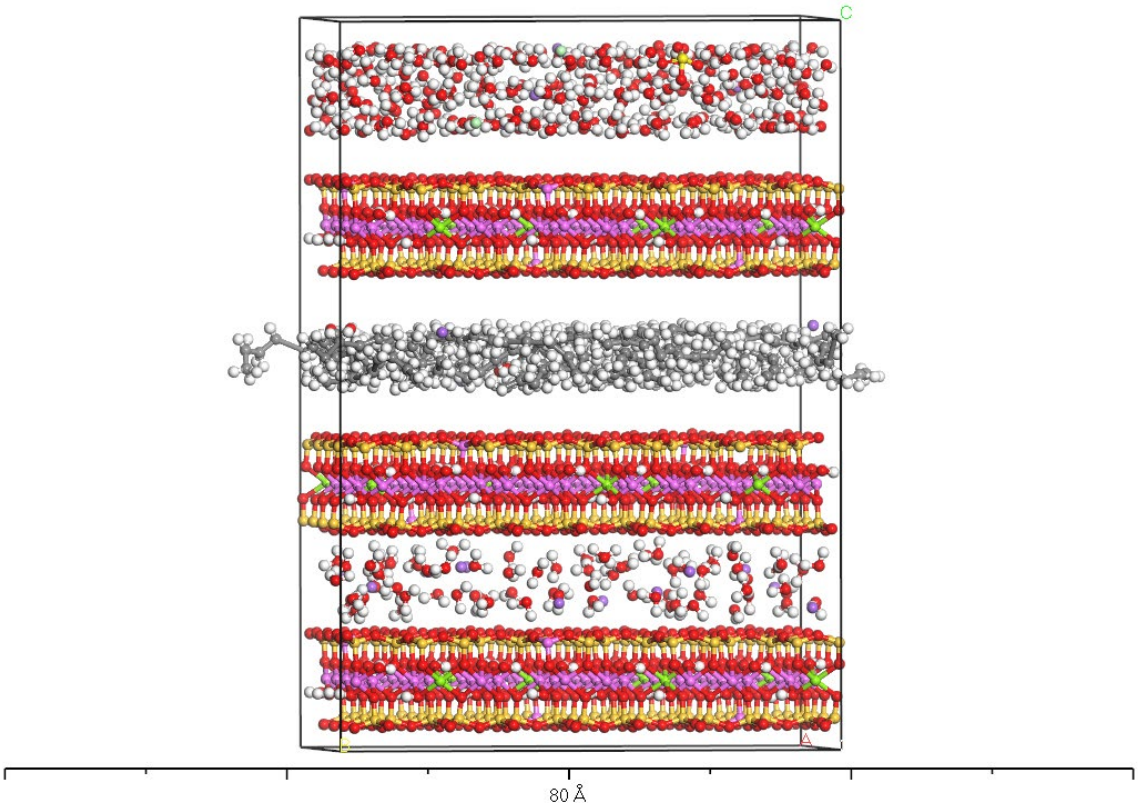

Figure 12. Snapshot of one of the initial Na-montmorillonite systems generated with water content corresponding to 5 H2O per unit cell, 30 decane with 4 polar protonated decanoic acid, and LSW (2-layer hydrate).

Three scenarios were generated using the system consisting of 48 unit cells, where the main idea was to predict the increase in basal d-spacing. Those scenarios were varying with different ion concentrations. The parameters with ion concentration will be discussed below.

The consensus of choosing Na-montmorillonite for this study is because of the surface negative charge which can adsorb acids in the oil and it tends to be the most swelling and problem causing clay, also in contrast of other clays, it has high cation exchange capacity (CEC) of 2:1 which has a significant role in low salinity waterflooding.

Since system corresponds to the existing experimental samples on water content and layer spacing the intercalated 64 water molecules corresponding to 0.088 g_{H2O}/g_{clay} represented 2W hydration state with approximately 15 Å of basal d-spacing with 12 Na^+ cations are incorporated into the system to balance the negative surface charge of Na-montmorillonite. The salinity of formation water with 64 water molecules and 12 Na^+ ions represented nearly 240,000 ppm and according to Jerauld et al., (2008) the salinity was selected to be between 25,000 ppm and 60,000 ppm. The different scenarios of LSW were modelled with a varying salt concentration, more specifically ion concentrations of Na, Cl and SO_4 at water content of 256 atoms as shown in Table 5. The LSW layer was built through the amorphous cell function provided by Materials Studio and one of the scenarios was provided in the Figure 13 below.

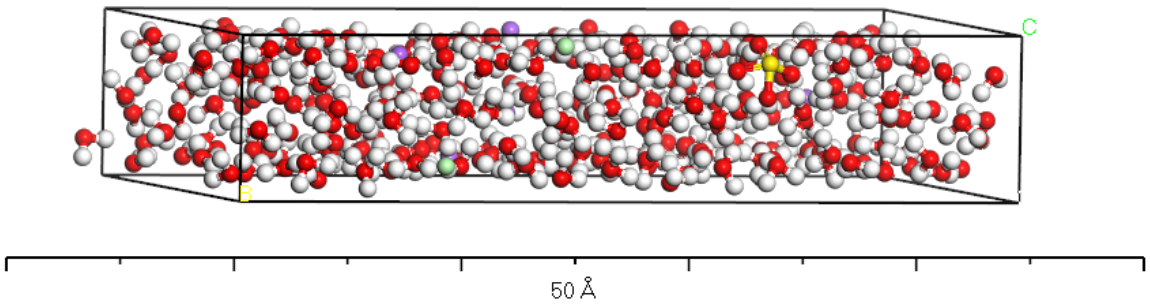

Figure 13. The layer of LSW for the system S1.

According to Peng et al., (2019) the contribution of exchangeable cations decreases as a number of water molecules increase. Thus, in this study we pay more attention to the exchangeable cations which are the major ions on LSW rather than number of water molecules.

Table 5. System properties with salt concentration

System	Solvent	Salt	Number of salt molecules	Concentration
S1	Water	$Na^+ + Cl^-$	9 + 2	60,000 ppm
S2	Water	$Na^+ + Cl^-$	4 + 2	35,000 ppm
S3	Water	$Na^+ + Cl^-$	2 + 2	25,000 ppm

4.2 The Organic Molecules model

The organic molecules used in this study were non-polar decane ($C_{10}H_{22}$) and charged sodium decanoate $Na^{+}(CH_3(CH_2)_8COOH)^{-}$ which can exemplify such mechanisms as multi-component ion exchange and electric double layer expansion. The oil layers were generated by the Amorphous cell function with an overall 30 decane and 3 charged decanoate with 12 counterbalance cations of sodium (Figure 14). This is because asphaltene aggregates such as toluene or n-heptane absorbed to the clay mineral represented the interlamellar volume of 15-16 Å (Pernyeszi et al., 1998).

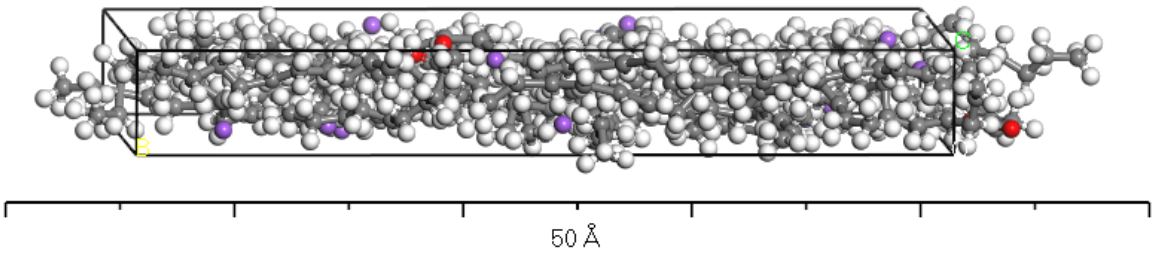

Figure 14. The Confined layer of crude oil with 30 non-polar decane and 3 charged sodium decanoate with 12 interlayer Na+ ions.

4.4 Simulation Parameters

There are many force fields in MD studies of low salinity waterflooding for at least three different force fields (clay, water and hydrocarbon) and there no exact restriction on using certain ones.

The consensus on using COMPASS force field as an all-atom force field is because it was tested and proved that it gives an accurate representation of most common organic and inorganic components. According to Sun et al., (1998) the COMPASS force field represented the most reliable and statistically appropriate results on density function of clay while showing good responses on both water and hydrocarbon. The equation of COMPASS force field is represented as follows:

$$E_{total} = E_{bond} + E_{angle} + E_{oop} + E_{torsion} + E_{cross} + E_{elec} + E_{l} \qquad (4)$$

where E_{oop}, $E_{torsion}$ and E_{cross} are the out-of-plane angle coordinates, bond torsion energy, and cross coupling interacting energy.

4.5 Simulation Details

All the simulations were carried out using Forcite module in the BIOVA Materials Studio 7.0 by Dassault Systèmes with the electrostatic and van der Waal cut-off distance of 1.25 nm which represents Medium quality during the simulation. The numerical integration method here was used the Verlet integration to calculate the trajectories of particles in molecular dynamics and to describe Newton's equation of motion. The step wise procedure of this simulation work is illustrated in the flow chart below (Figure 15).

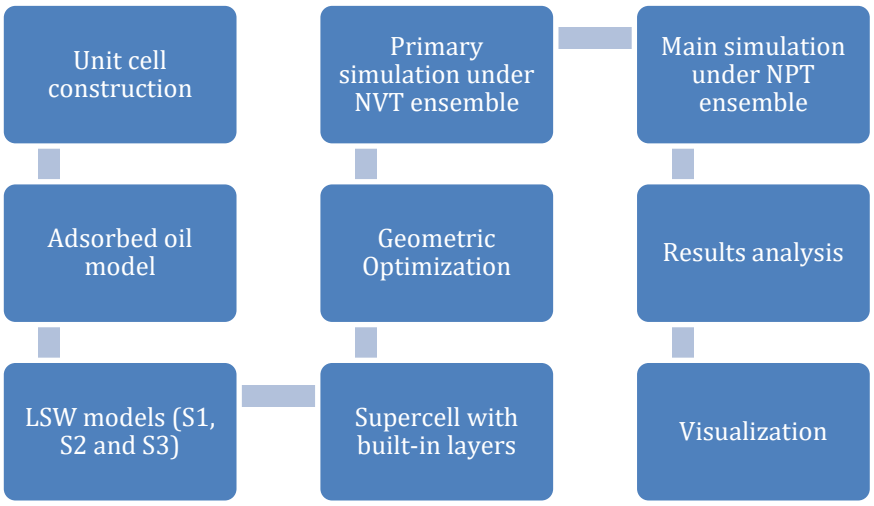

Figure 15. Flow chart of research methodology

After the geometrical optimization, the 50 ps production run with NVT ensemble with a timestep of 0.01 fs and the clay layers were fixed to achieve an initial condition of oil-wetness and equilibrate the system. Using the basic parameters provided by the COMPASS force field such as Ewald electrostatic at buffer width of 0.5 Å and Ewald accuracy of 0.001 kcal/mol, van der Waals as atom-based where the Truncation was selected as a cubic spine and cutoff distance of 12.5 Å, and the buffer width 0.5 Å and Spline width 1 Å. After allowing every atom to move the simulation was run by the 1.5 ns which was enough to extract reasonable results from water self-diffusion coefficient at T=330 K and P=1 bar for each salt concentration in the NVP ensemble with a pressure coupling set at 1 ps in semi-isotropic barostat, and temperature coupling constant of 0.1 ps in velocity rescale thermostat.

The simulation was wrapped up with the last 50 ps of analysis run to generate the required data and graphs, such are layer spacings, density profiles and radial distribution functions and so on which will be described in the results chapter of this thesis work.

4.6 Visualization

All the snapshots were taken from Materials Studio 7.0 by Accelrys itself. All simulations were carried out on the identical triple Na-montmorillonite layer with varying salinity (S1-S3). The color scheme of every snapshot provided above is described such that, silicon (yellow), aluminum (purple), magnesium (green), oxygen (red), sodium (light purple), chlorine (teal) and hydrogen (white) atoms, while for the organic molecules it is a carbon (grey), oxygen (red), and hydrogen (white). All the color schemes were kept the same except the unit cell where the legend was given already.

5. RESULTS AND DISCUSSION

In this chapter the results obtained from this study are presented. These results are extracted from trajectory data file of the simulations of NVT and NPT ensemble with varying salinity. The primary scenario where the main objective was to predict clay swelling effect results included the layer spacing (distance between the clay layers), density profile, and hydration energy (energy transition between the layers).

5.1 System equilibration

After the 50 ps of production run followed by the 1.5 ns simulation hours the system was stabilized and reached equilibrium. According to the graphs presented below for each LSW system (S1-S3), the first indication of equilibration is from the Energy profile where the constant value has been achieved resulting the same value over all system (Figures 16-18).

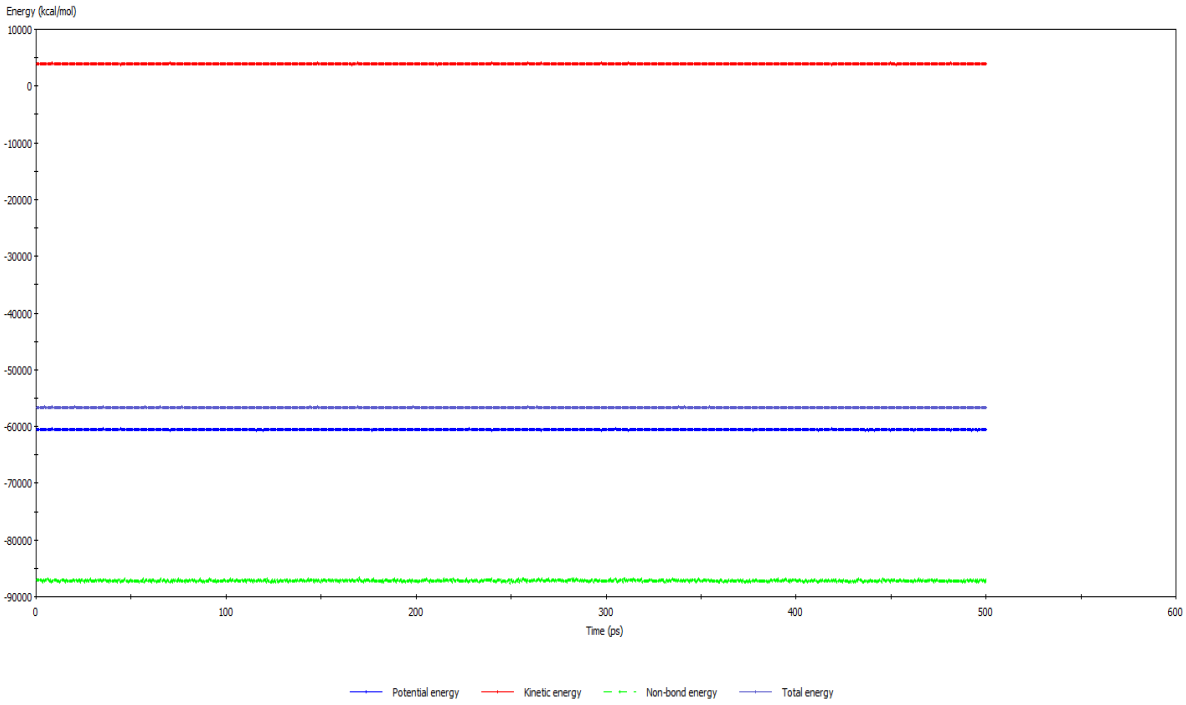

Figure 16. Energy profile for the system S1

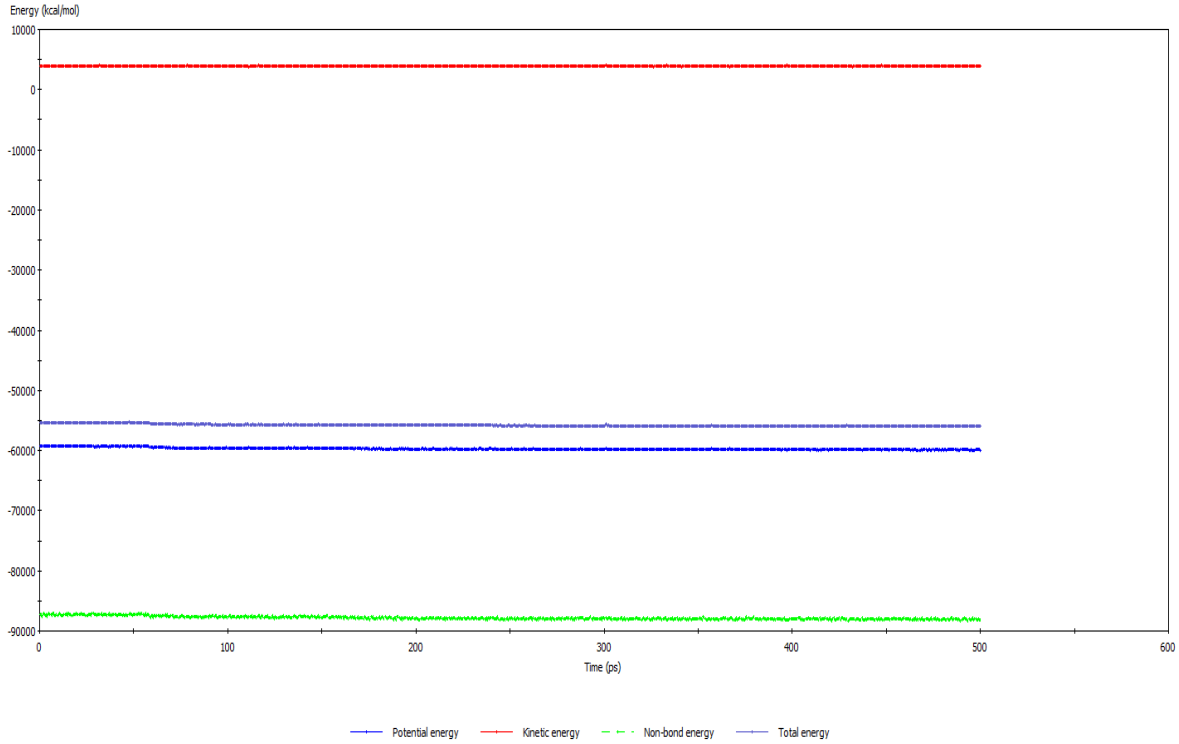

Figure 17. Energy profile for the system S2

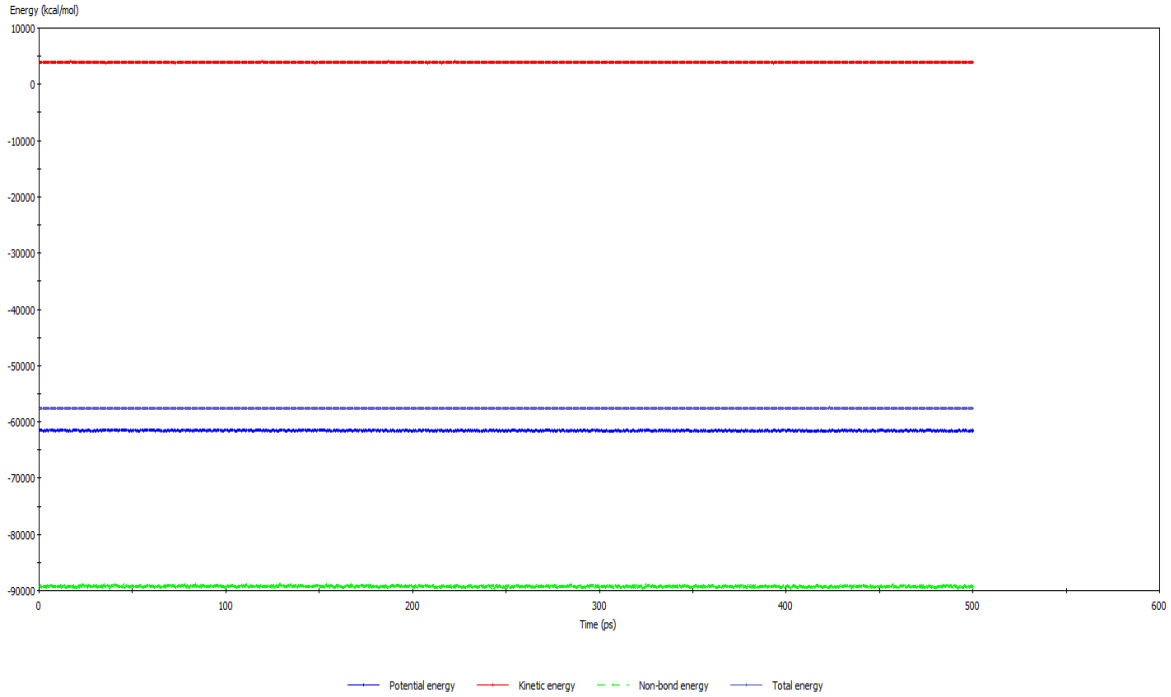

Figure 18. Energy profile for the system S3

The temperature profiles show expected responses for all the system under given value of T=330 K as an initial temperature and as it can be seen the values are fluctuation around the initial value which means that the equilibrium has been reached (Figures 19-21).

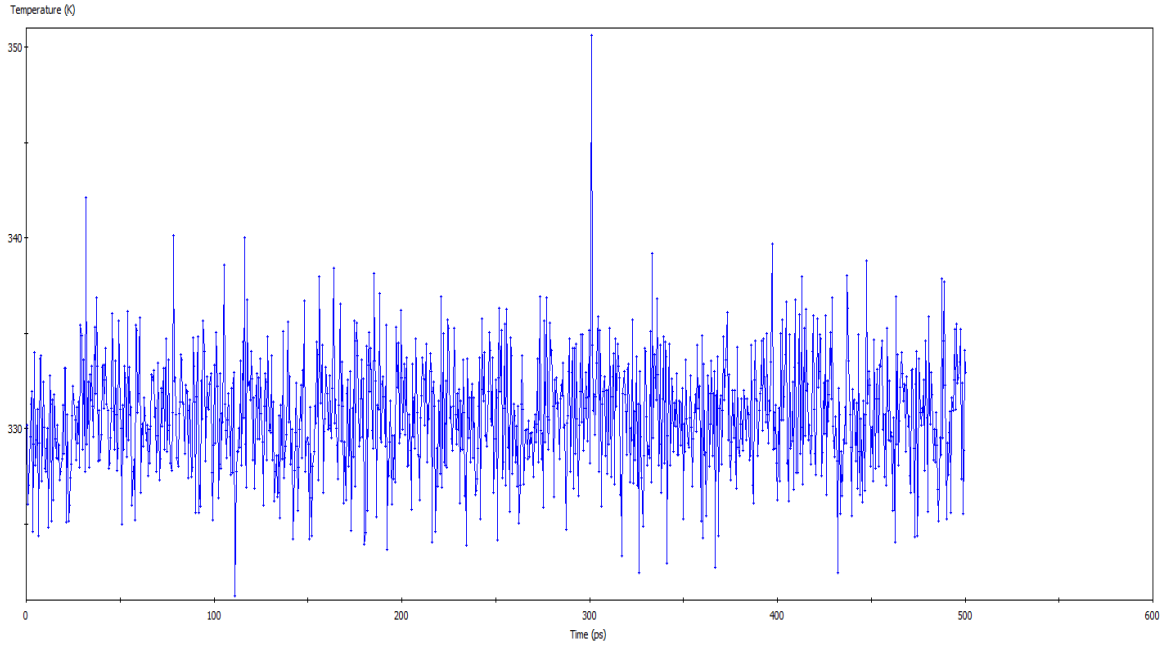

Figure 19. Temperature profile for the system S1

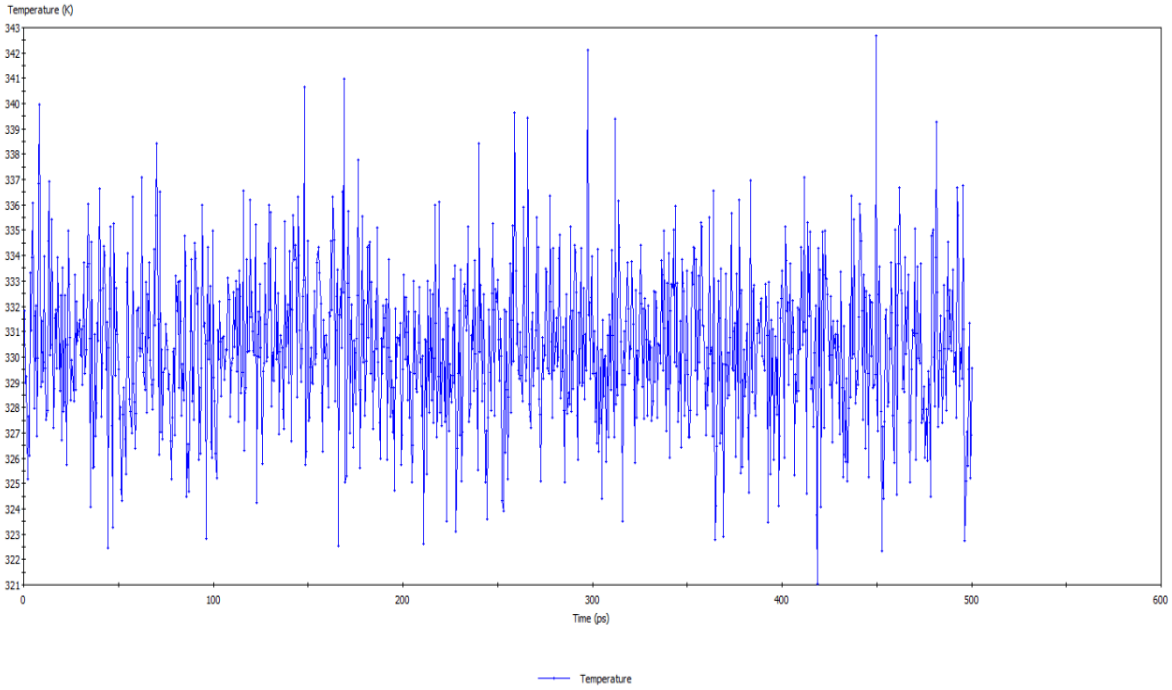

Figure 20. Temperature profile for the system S2

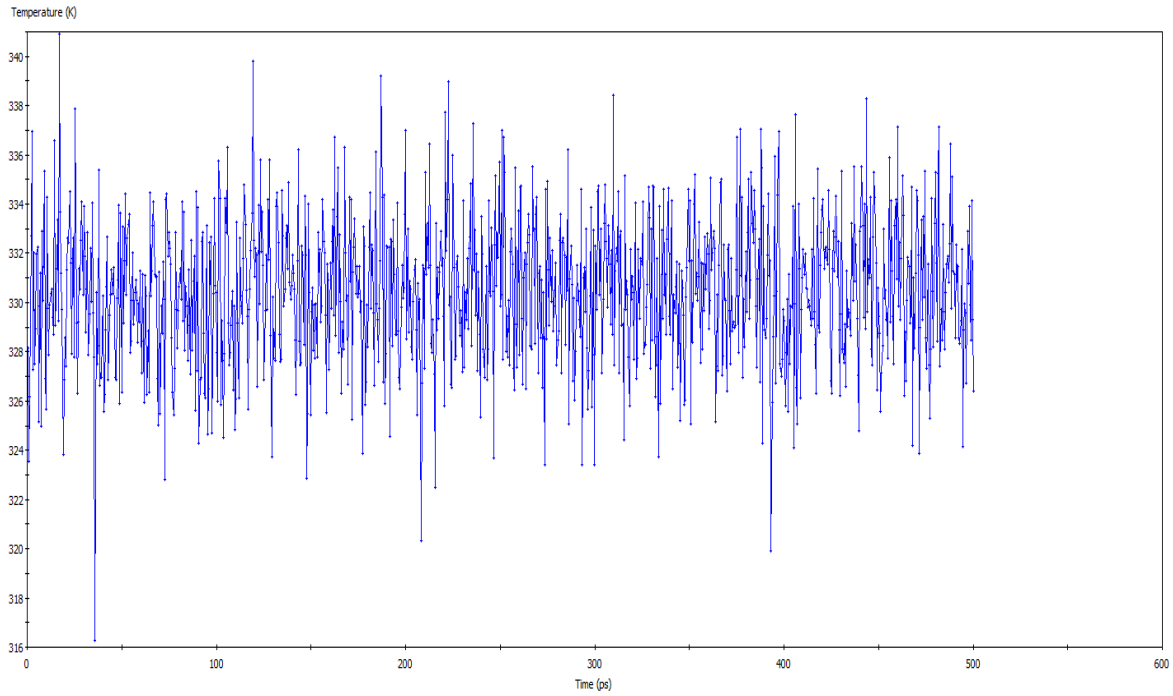

Figure 21. Temperature profile for the system S3

5.1.1 Layer Spacing

After the NPT simulation runs were finished the basal d-spacing as a function of water content was calculated which the direct indication of system volume change depending on the hydration adjustments. The equation for the basal d-spacing calculation is as follows:

$$d = \frac{\langle a \rangle \langle b \rangle \langle c \rangle}{2\langle a \rangle \langle b \rangle} = \frac{\langle c \rangle}{2} \tag{5}$$

where a, b and c are the dimensions of the simulation system.

$$d = \frac{31.686}{2} = 15.843 \tag{6}$$

$$d = \frac{32.392}{2} = 16.196 \tag{7}$$

$$d = \frac{34.248}{2} = 17.124 \tag{8}$$

The resulting basal d-spacing for initial 15 Å state exhibits the distance of 15.843 Å for the system S1, while the layer spacing for the S2 is 16.196, and S3 executed the spacing of 17.124 Å. As expected that the results from the simulations demonstrate the tendency of swelling on every salt concentration as shown in the following figure. Although, the scale of swelling is different for each system with different layer spacing. According to Figure 22, the

layer spacing is the biggest among other systems which correspond to the S3 and the general trend of layer spacing increases as a salt concentration of LSW decreases due to the low number of counterions located. Between the scenarios S3 and S1 there is a large difference and fluctuation can be seen in interlayer spacing, while S2 exhibits relatively smaller layer spacing in comparison with S3. This phenomenon can simply be explained by the theory which was mentioned before that the clay swelling properties directly depends on interlayer cations that are meant to counterbalance negative surface charge of clay layer and due to the lower number of ions located in LSW, intake of Na^+ ions located in higher ion concentration will happen in order to balance the ion concentration among the clay layers. This is further developed and the free unbounded ions will attract water molecules and absorb them and increase interlayer spacing. Summing up, the system consisting of highest number of counterions among other systems, the system S1 is the most relevant LSW with optimum salt concentration.

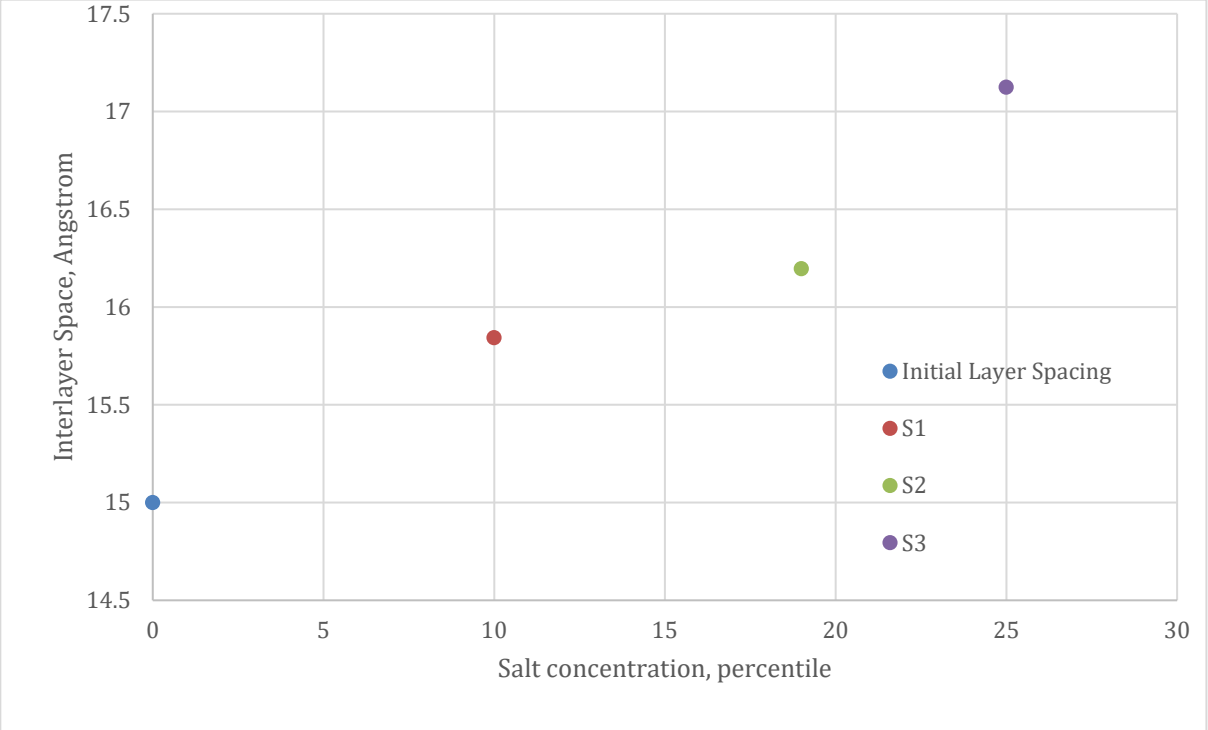

Figure 22. Interlayer Space profile for the Na-MMT at three different salt concentrations

5.1.2 Density profile

Usually, in the interlayer of clay mineral, there are two types of complexes, inner-sphere which are formed when there are no water molecules between the cation and clay surface and outer-sphere where there is at least one water molecule present in between. The generation of complexes directly depends on the layer charge of clays. Such as having a layer charge located in the octahedral layer can create outer-sphere complexes, while in case of layer charge located

in the tetrahedral layer the inner-complexes can be seen. There are both inner-sphere and outer-sphere complexes present in Na-montmorillonite due to the layer charge located in both tetrahedral and octahedral layers. Therefore, initially, Na-montmorillonites are stable, although after the injection of any type of water in terms of salinity, the system gets disturbed and the number of complexes increase or decrease, respectively.

In order to determine the swelling property of the clay three density profiles of LSWF has been selected to analyze the structural and dynamical behavior of the clay interlayer. The density profile or in other words relative concentration shows the probability of finding certain atom types along the c-axis of the system at distance z from the surface. Figures 23-25 represent the density profiles for three different low salinity water composition, namely S1, S2, and S3 the salt content of which was given in Table 5 above. According to Figure 23, the sphere complexes are separated into two regions indicated with a number of 1 which is inner-sphere, while the region 2 with is outer-sphere is not present due to the fact that there are no small bumps after the first region.

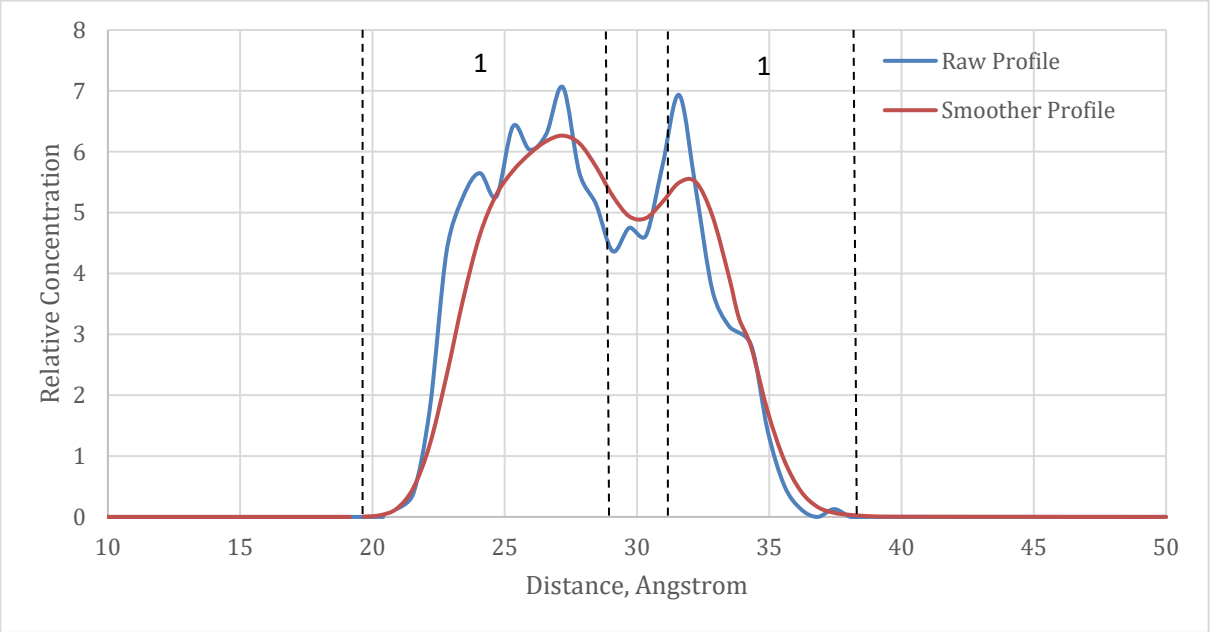

Figure 23. Concentration profile of LSW layer for the system S1

The identification sphere complexes are directly related to the layer spacing, for instance, if the distance from the surface varies between 8 and 10 Å then there are inner-sphere complexes, while for the outer-sphere complexes it is 4-4.5 Å beyond inner-sphere complexes which in this case are not present. According to Figure 23, we can see the presence of inner-sphere for the 256 water molecules intercalated with a various number of Na^+ ions. A high number of inner-sphere complexes are the responsible ones on triggering the effect of clay

swelling, in case of the formation water layer, instead, the number of outer-sphere complexes will be more. This is due to the mechanism causing clay swelling where the tendency of intercalated cations to transfer to the layer of lower cation concentration. The relative concentration of inner-sphere complexes is rising gradually from S1 to S3, this means that the system S3 has the highest tendency of swelling.

Regarding the peak, in case of intercalated formation water the peak in wider on region 1, which indicated a large number of inner-sphere complexes and the system S2 has relatively wider area of region 1 (Figure 24). Although, in system S3 there is a small indication of outer-sphere complexes present and it is a relatively narrow peak with a smaller number of outer-sphere complexes.

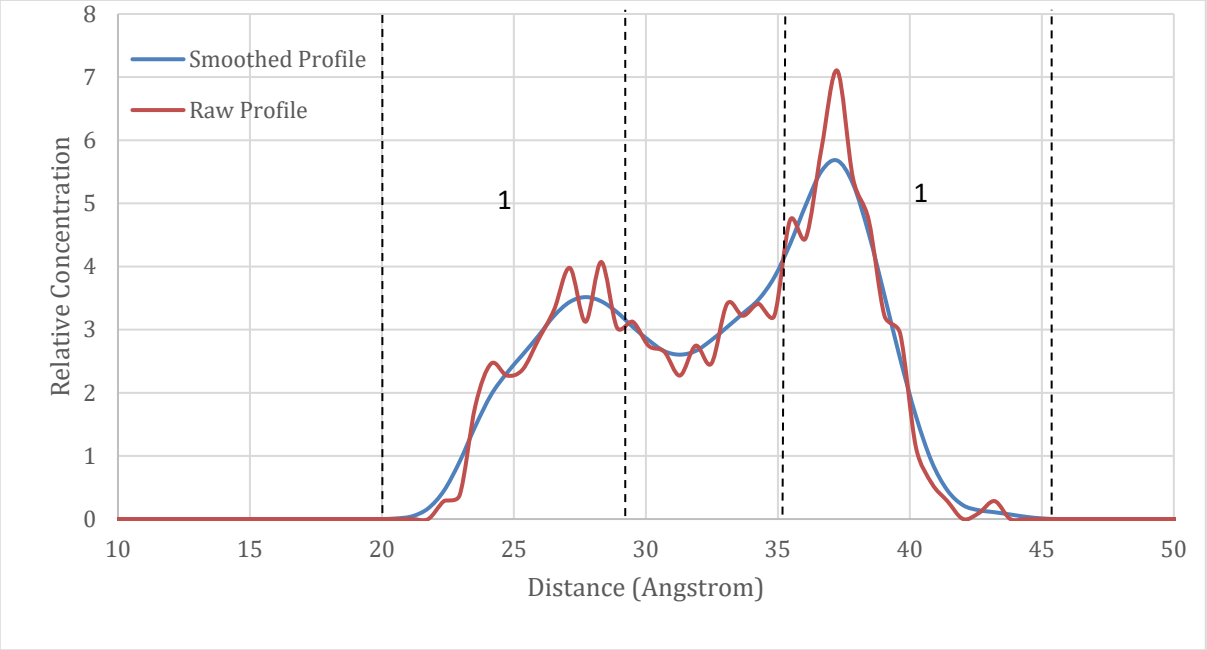

Figure 24. Concentration profile of LSW layer for the system S2

According to density profiles of the system S3, there can be seen three peaks at different locations, which is due to the excessive number of water molecules that is capable of generating central peak slipping two peaks (Figure 25). This phenomenon can be explained by the effect of diffuse ion swarm in which the exchangeable cations are located close basal plane and attracted to them, even though they remain separated from the surface. This can be caused, again, due to the not sufficient amount of interlayer cations present in neighbor basal space.

Following the effect caused by the diffuse ion swarm, the arrangement of water molecules will be more spread out from the midplane of the spacing.

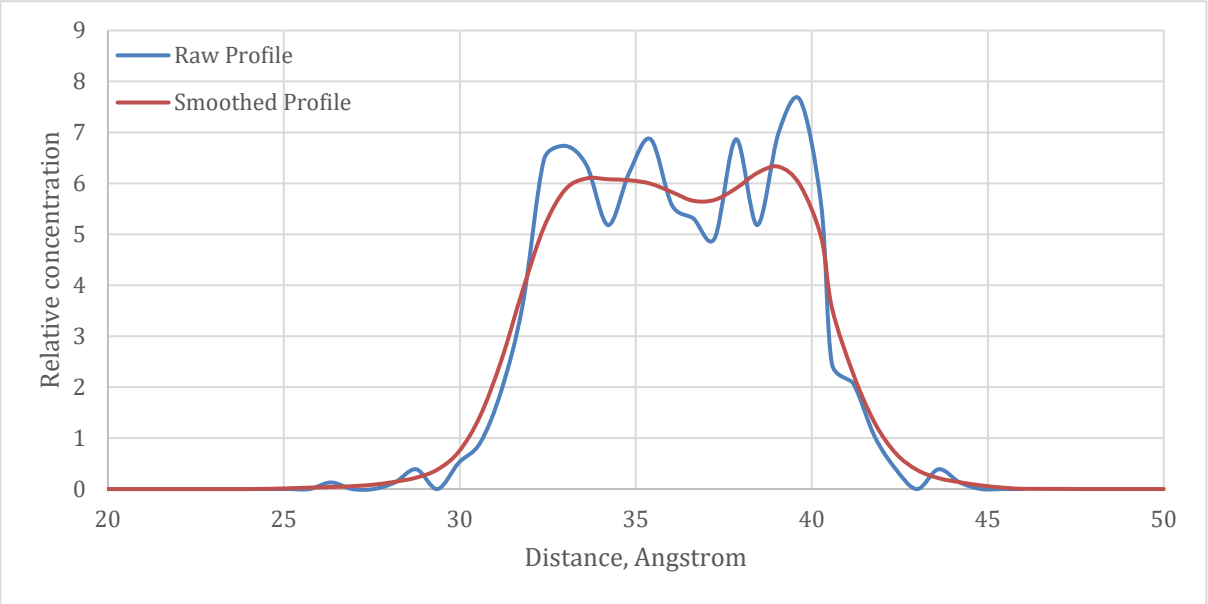

Figure 25. Concentration profile of LSW layer for the system S3

Finally, it is quite obvious if we analyze according to the interlayer distance. The wider the distance located higher concentration of low salinity water leads to the swelling effect or in other words increase of interlayer space. According to the Figures 23-25, the tendency of increasing of space between the two clay mineral layers, respectively. The system S1 has the lowest interlayer space and increases gradually for the system S2 then to the S3.

5.1.3 Radial Distribution Functions

It is prerequisite to perform analysis on radial distribution functions after the density profile which represents the probability of finding a particle at a certain distance from the clay surface. In this study, RDF profiles were generated first one is between the clay surface and LSW for the systems S1, S2 and S3 three LSW compositions (Figures 26-28). The cutoff distance for the RDF between clay surface and LSW was selected to be 5 Å which can include both first hydration layer and Stern layer of the clay surface, while the same cutoff distance of 5 Å was also capable of representing RDF between the water molecules and cations. The first-neighbor peak for the S1 system is started at 1.015 Å and centred at 1.105 Å while for the upcoming systems S2 and S3 the locations of the first peak are approximately similar. Although, the centred peak location for the system S1 is relatively bigger and more concentrated in comparison with other systems S2 and S3. This can be explained by the number of interlayer

cations present in the system and the shift is due to the low number of exchangeable cations present in the system.

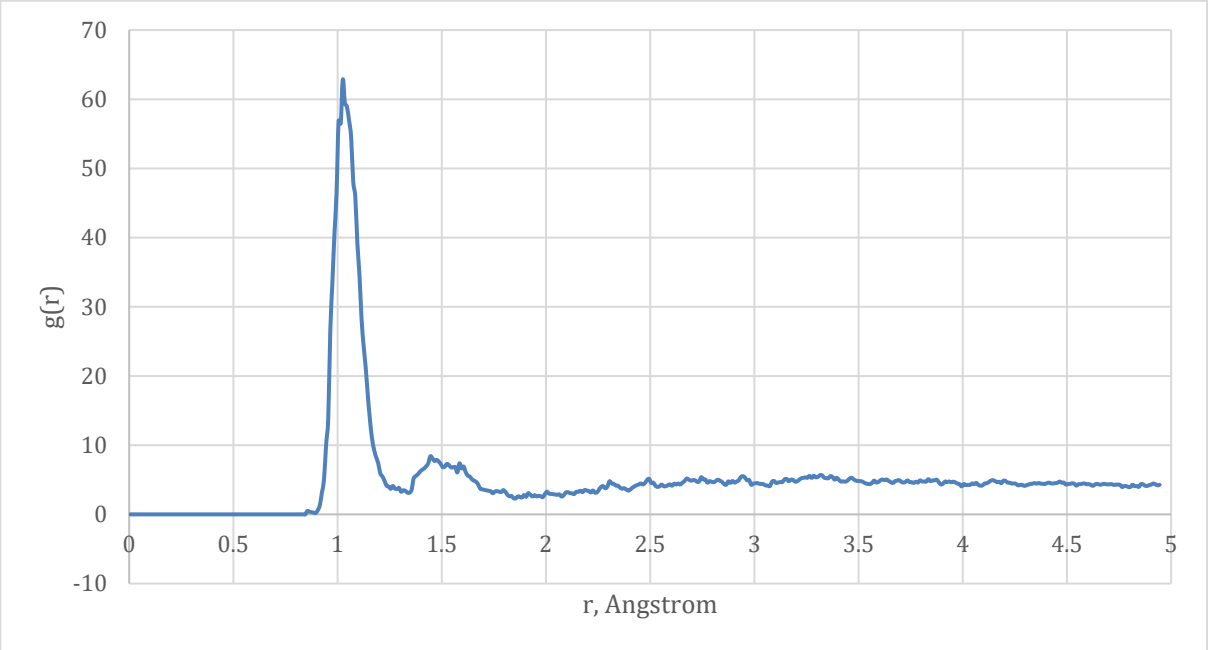

Figure 26. Radial Distribution Function for the system S1

The following neighbor peaks are present for all system and they are relatively high although and the hydration shell for the systems S2 and S3 are similar and the abundancy is higher than the system S1 which is due to the fact of not sufficient amount of interlayer cation (Na^{+}). The compact hydration shell for the second and third neighbor peaks are assembled more densely for the S3 and S2 in comparison with S1 which is again due to the number of interlayer cation.

In general, there is a theory that tells about the decrease in the hydration of ions in the aqueous solution with the increase in salinity (Zhao et al.). Therefore, the system S1 has been preferred as a good representative of LSW in this study causing less swelling and less hydration of ions.

The swelling effect is identified from all the systems, although the degree of swelling is decreased in the order of S3 then S2 and finally, S1. Finalizing the results from the analysis of RDF the driving force for the swelling is caused by the fully hydrated exchangeable ions. The reason for selecting S3 as the most swelling system is due to the fact than less number of counterion the initial interlayer with the number of 256 water molecules the counterions get fully hydrated and allocate themselves in the mid plane of the interlayer, while the transferring initially single or two shelled exchangeable ions interact with the clay mineral surface and

hydrate further until the bulk limit is reached. Overall, the reason for such big correlation factor (y-axis) could be explained by the number of water molecules for such small system.

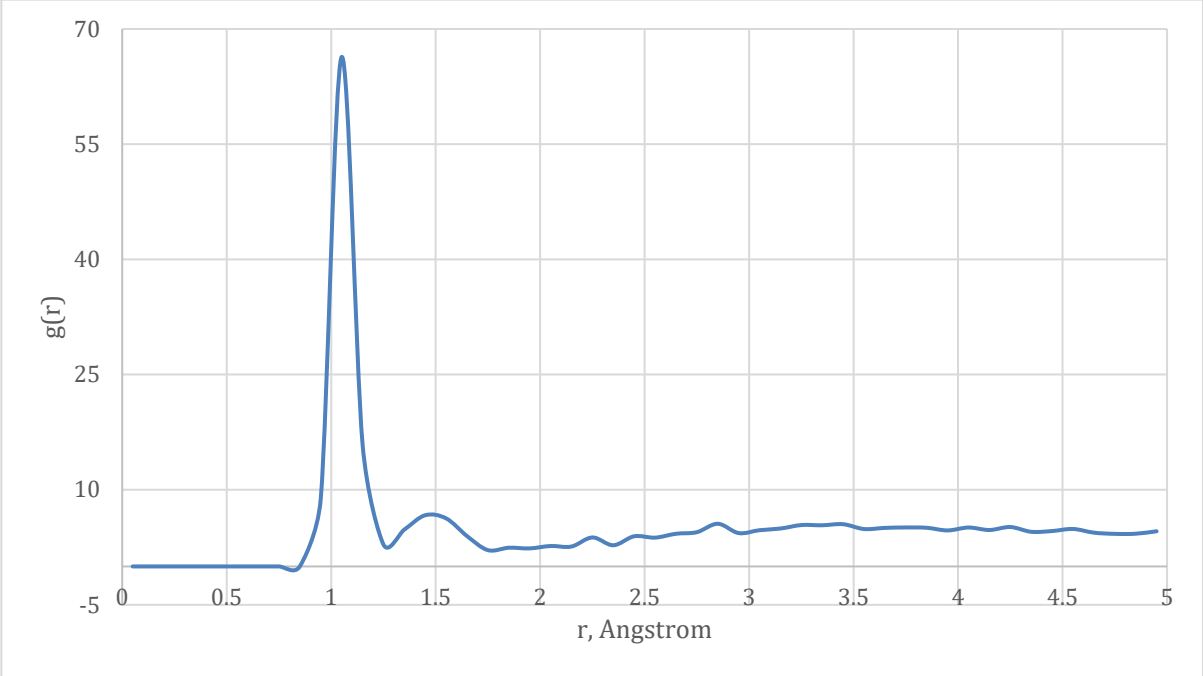

Figure 27. Radial Distribution Function for the system S2

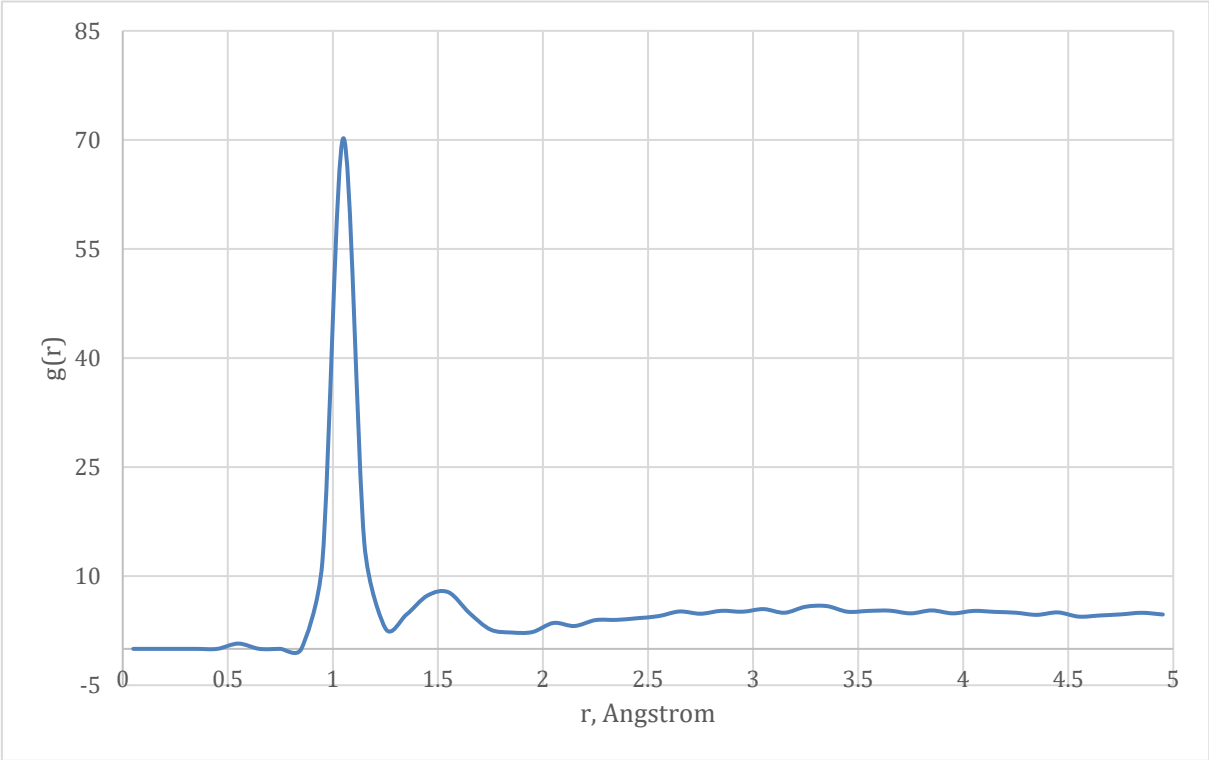

Figure 28. Radial Distribution Function for the system S3

5.1.4 The Hydration Energy

The hydration energy of Na-montmorillonite is relatively smaller than other types of clays and this leads to the relatively bigger interlayer space. The hydration represents the energy change due the transition of water in the hydrated layer towards the layer with lower hydration or dry layer which can be calculated by following equation:

$$\Delta U = \frac{\langle U\langle N\rangle\rangle - \langle U\langle 0\rangle\rangle}{N} \tag{9}$$

where $\langle U\langle N\rangle\rangle$ and $\langle U\langle 0\rangle\rangle$ are the potential energies of the hydrated and aver, while N is the number of interlayer water molecules. The representation of dry layer was selected to the initial interlayer formation water and average potential energy was calculated to be 16.17885 kcal/mol, while as a hydrated layer was selected LSW layer and the hydration energy was calculated in the equations 10-12. The plot of hydration energy against the LSW with different ionic composition was built (Figure 30).

$$\Delta U_{S1} = \frac{-6089.4739 - 16.17885}{256} = -23.8502 \tag{10}$$

$$\Delta U_{S2} = \frac{-7359.3285 - 16.1789}{256} = -28.8106 \tag{11}$$

$$\Delta U_{S3} = \frac{-8211.99006 - 16.1789}{256} = -32.1413 \tag{12}$$

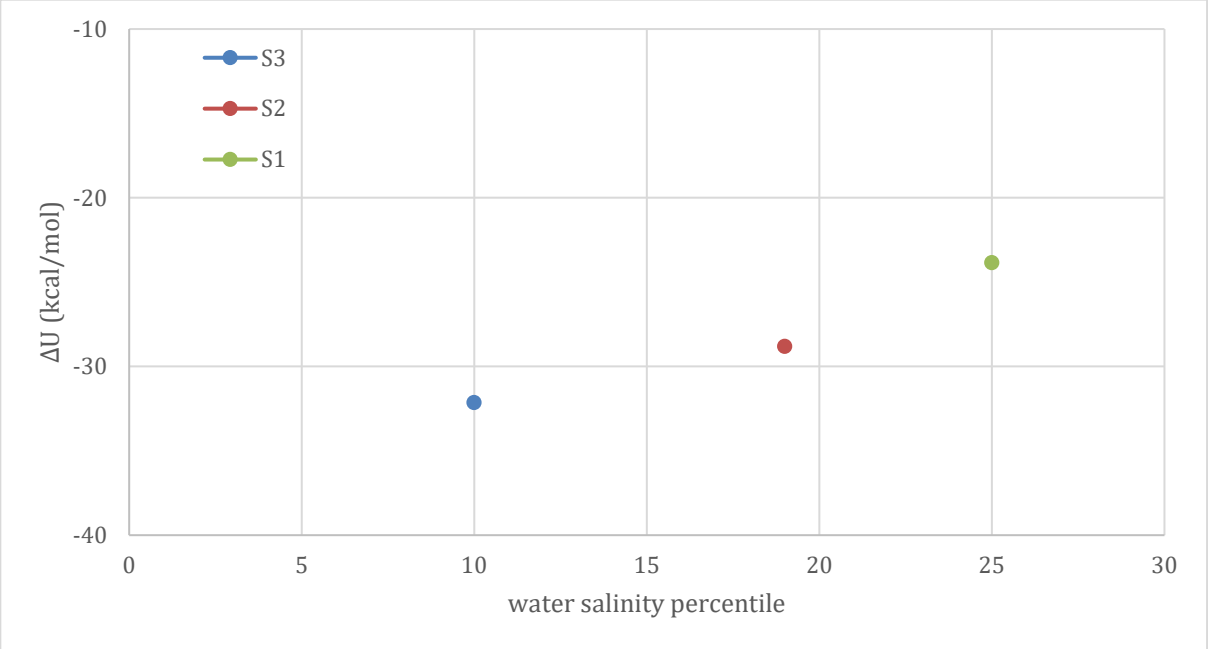

Figure 30. Hydration energy curve for Na-montmorillonite simulated with three different LSW models

A comparison between our three systems S1-S3 shows that the hydration energy for the system S1 has the highest value at the fixed water content of 256 molecules or 0.088 g_{H2O}/g_{clay} while the other systems followed gradual decrease in order of S2 and S3, respectively. These findings again confirm the results gathered from the layer spacing, density profile and the RDF that the number of exchangeable cations present in water layer dictate a lot on the swelling effect of Na-montmorillonite mineral.

5.1.5 Na decanoate effect on Na-montmorillonite

Finally, in order to confirm the effect of organic molecules such as charged sodium decanoate on Na-montmorillonite to generate initial condition of oil-wetness the density profile analysis has been conducted using the Materials Studio. The density profile graph provided below describes the attachment of sodium decanoate to the dry interlayer of Na-montmorillonite (Figure 31).

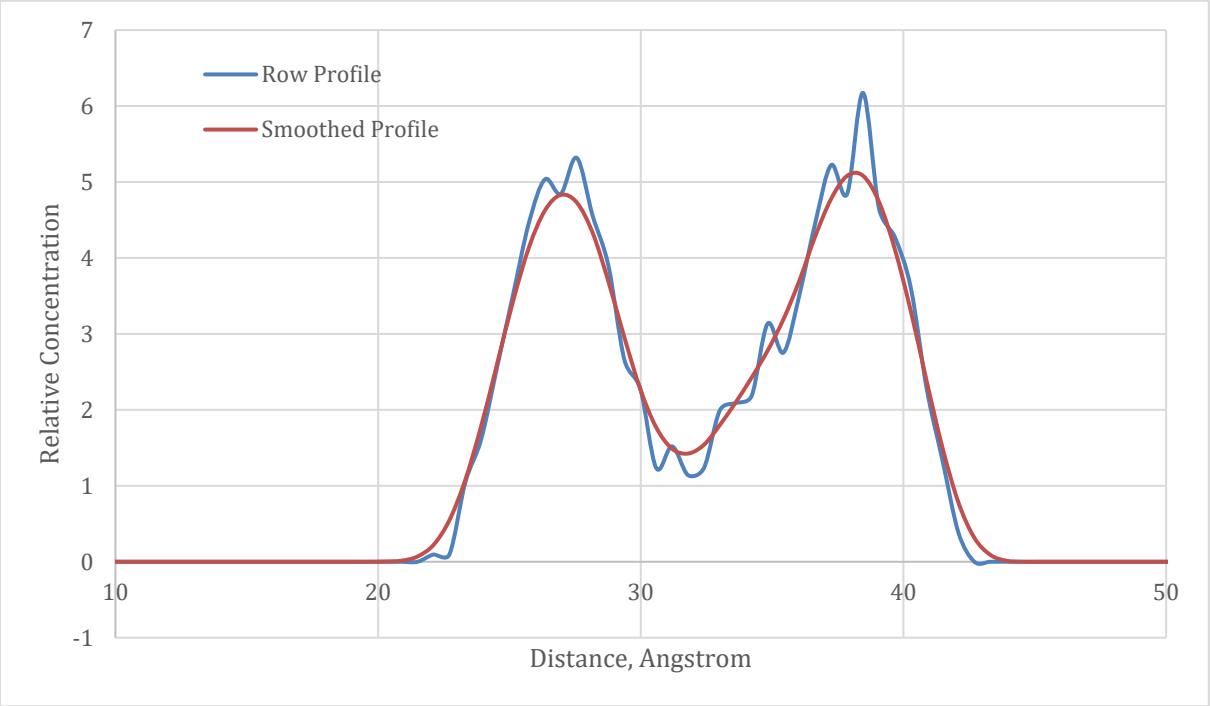

Figure 31. Concentration profile of crude oil layer for all the systems

According to the concentration graph the distribution of oil layer is closer to the clay site of the system which is quite obvious that the initial condition has been generated. It is clear that due to the charged organic molecules with divalent ions in this case it is sodium, the state of oil-wetness has been achieved. This can be explained by the protonation of charged sodium decanoate in the crude oil.

6. CONCLUSIONS AND RECOMMENDATIONS

In this chapter the conclusions of the simulation with the final verdict and the recommendations for the future work are provided.

6.1 Conclusions

The use of molecular dynamics simulations has helped us investigate at molecular scale the effect of injection of LSW into clay bearing sandstone reservoirs causing clay swelling effect. The objectives of this research were to study the effect of LSWF causing swelling of clay minerals present in sandstone reservoirs. According to the findings from this molecular dynamics simulations study following 5 conclusions can be drawn.

1. The presence of pure Na-montmorillonite in sandstone reservoirs is the appealing scenario to attract the charged components in hydrocarbon for the LSWF due to the net negative surface charge executing from both octahedral and tetrahedral layers. This was achieved by the substitutions in each layer.

2. Presence of charged divalent cations in crude oil or organic acids is the primary requirement for the generation of the initial condition and most likely suitable scenario for the injection of low salinity water due to the displacement of divalent ions with monovalent ions.

3. The molecular-level insights of clay analysis showed the presence of water with lower salt concentration than the formation brine can trigger the effect of swelling. The results indicate that the usage of LSW at 25% of original salinity is the most likely to bypass the problem of permeability impairment while using the 10% of salinity triggered that effect and hydrocarbon layer in between decreased its size which is not the desired result.

4. An insufficient number of exchangeable cations between the interlayers of clay mineral layers leads to the phenomenon of diffuse ion swarm and allocate close to basal plane and attracted to them, even though they remain separated from the surface generating inner-sphere complexes.

5. The number of hydration shell around the Na^+ ions is directly related to the salinity of the water injected. The decrease in the hydration of ions in the aqueous solution with the increase in salinity (first, second, third and fourth shell) which means high salinity water injected can reduce the number of shells. This finalizes the optimum value of LSW at 25% or 60,000 ppm of initial formation brine.

It worth mentioning here that the results were obtained from specific conditions and may not show similar responses for other systems with different parameters and size.

6.2 Recommendations

Based on the results of this study it is recommended that further investigation be undertaken with respect to water content and layer hydration state. There could be done variety of studies for different hydration layers such as dry clay, 1W, 3W and 4W layers with relatively changing also number of water molecules with respect to the salinity. Another option is to increase the simulation hours 2-10 ns to get absolutely accurate and reliable numbers and longer simulation hours to reach state of equilibrium. Further optimization can be done on present COMPASS force field using quantum chemical calculations. Finally, use LSW of system S1 and simulate oil detachment from the initially oil-wet clay surface.

REFERENCES

Aitken, C. M.; Jones, D. M.; Larter, S. R. Anaerobic Hydrocarbon Biodegradation in Deep Subsurface Oil Reservoirs. *Nature* 2004, 431, 291−294.

Austad, T., & Standnes, D. C. (2003). Spontaneous imbibition of water into oil-wet carbonates. *Journal of Petroleum Science and Engineering*, 39(3-4), 363-376.

Austad, T., RezaeiDoust, A., & Puntervold, T. (2010, January). Chemical mechanism of low salinity water flooding in sandstone reservoirs. In *SPE Improved Oil Recovery Symposium*. Society of Petroleum Engineers.

Barratt, M. D. (1996). Quantitative structure-activity relationships (QSARs) for skin corrosivity of organic acids, bases and phenols: principal components and neural network analysis of extended datasets. *Toxicology in vitro*, 10(1), 85-94.

Brady, P. V., & Krumhansl, J. L. (2013). Surface complexation modeling for waterflooding of sandstones. *SPE Journal*, 18(02), 214-218.

Chávez-Páez, M., Van Workum, K., De Pablo, L., & de Pablo, J. J. (2001). Monte Carlo simulations of Wyoming sodium montmorillonite hydrates. *The Journal of Chemical Physics*, 114(3), 1405-1413.

Cygan, R. T., Liang, J. J., & Kalinichev, A. G. (2004). Molecular models of hydroxide, oxyhydroxide, and clay phases and the development of a general force field. *The Journal of Physical Chemistry B*, 108(4), 1255-1266.

Energy Information Administration (U.S.) and Government Publications Office. International Energy Outlook: 2018 with Projections to 2050. *International Energy Outlook*. U.S. Government Printing Office, 2019.

Fathi, S. J., Austad, T., & Strand, S. (2010). “Smart water” as a wettability modifier in chalk: the effect of salinity and ionic composition. *Energy & Fuels*, 24(4), 2514-2519.

Fazelabdolabadi, B., & Alizadeh-Mojarad, A. (2017). A molecular dynamics investigation into the adsorption behavior inside {001} kaolinite and {1014} calcite nano-scale channels: the case with confined hydrocarbon liquid, acid gases, and water. *Applied Nanoscience*, 7(5), 155-165.

Fink, D. H., & Thomas, G. W. (1964). X-Ray Studies of Crystalline Swelling in Montmorillonites. *Soil Science Society of America Journal*, 28(6), 747-750.

Greathouse, J. A., Cygan, R. T., Fredrich, J. T., & Jerauld, G. R. (2017). Adsorption of aqueous crude oil components on the basal surfaces of clay minerals: molecular simulations including salinity and temperature effects. *The Journal of Physical Chemistry C*, 121(41), 22773-22786.

Hamouda, A. A., Valderhaug, O. M., Munaev, R., & Stangeland, H. (2014, April). Possible mechanisms for oil recovery from chalk and sandstone rocks by low salinity water (LSW). In *SPE Improved Oil Recovery Symposium*. Society of Petroleum Engineers.

Jadhunandan, P. P., & Morrow, N. R. (1991). Spontaneous imbibition of water by crude oil/brine/rock systems. *In Situ*; (United States), 15(4).

Jadhunandan, P. P., & Morrow, N. R. (1995). Effect of wettability on waterflood recovery for crude-oil/brine/rock systems. *SPE Reservoir Engineering*, 10(01), 40-46.

Jerauld, G. R., Webb, K. J., Lin, C.-Y., & Seccombe, J. C. (2008, December 1). Modeling Low-Salinity Waterflooding. *Society of Petroleum Engineers*.

Kakati, A., Kumar, G., & Sangwai, J. S. (2020). Oil Recovery Efficiency and Mechanism of Low Salinity-Enhanced Oil Recovery for Light Crude Oil with a Low Acid Number. *ACS Omega*.

Katende, A., & Sagala, F. (2019). A critical review of low salinity water flooding: mechanism, laboratory and field application. *Journal of Molecular Liquids*, 278, 627-649.

Kulkarni, M. M., & Rao, D. N. (2005). Experimental investigation of miscible and immiscible Water-Alternating-Gas (WAG) process performance. *Journal of Petroleum Science and Engineering*, 48(1-2), 1-20.

Lager, A., Webb, K.J., and Black, C.J. 2006. Low Salinity Oil Recovery-An Experimental Investigation. Paper SCA 2006-36 presented at the *International Symposium of the Society of Core Analysts*, Trondheim, Norway, September.

Lee, S. Y.; Webb, K. J.; Collins, I. R.; Lager, A.; Clarke, S. M.; O'Sullivan, M.; Routh, A. F. Low Salinity Oil Recovery: Increasing Understanding of the Underlying Mechanisms. In *SPE*

Improved Oil Recovery Symposium; Society of Petroleum Engineers: Tulsa, OK, 2010; p SPE-129722-MS.

Ligthelm, D. J., Gronsveld, J., Hofman, J., Brussee, N., Marcelis, F., & van der Linde, H. (2009, January). Novel Waterflooding Strategy by Manipulation of Injection Brine Composition. In *EUROPEC/EAGE conference and exhibition*. Society of Petroleum Engineers.

Mahmud, H. B., Arumugam, S., & Mahmud, W. (2019). Potential of Low-Salinity Waterflooding Technology to Improve Oil Recovery. In *Enhanced Oil Recovery Processes-New Technologies*. IntechOpen.

Marhaendrajana, T., Ridwan, M. G., Kamil, M. I., & Permadi, P. (2018). Wettability Alteration Induced by Surface Roughening During Low Salinity Waterflooding. *Journal of Engineering and Technological Sciences*, 50(5), 635-649.

McGuire, P. L., Chatham, J. R., Paskvan, F. K., Sommer, D. M., & Carini, F. H. (2005, January). Low salinity oil recovery: An exciting new EOR opportunity for Alaska's North Slope. In *SPE Western Regional Meeting*. Society of Petroleum Engineers.

Meleshyn, A., & Bunnenberg, C. (2005). The gap between crystalline and osmotic swelling of Na-montmorillonite: A Monte Carlo study. *The Journal of Chemical Physics*, 122(3), 034705.

Mooney, R. W., Keenan, A. G., & Wood, L. A. (1952). Adsorption of water vapor by montmorillonite. II. Effect of exchangeable ions and lattice swelling as measured by X-ray diffraction. *Journal of the American Chemical Society*, 74(6), 1371-1374.

Morrow, N., & Buckley, J. (2011). Improved oil recovery by low-salinity waterflooding. *Journal of Petroleum Technology*, 63(05), 106-112.

Mwangi, P., Brady, P. V., Radonjic, M., & Thyne, G. (2018). The effect of organic acids on wettability of sandstone and carbonate rocks. *Journal of Petroleum Science and Engineering*, 165, 428-435.

Norrish, K. (1954). The swelling of montmorillonite. *Discussions of the Faraday Society*, 18, 120-134.

Omekeh, A. V., Friis, H. A., Fjelde, I., & Evje, S. (2012, January). Modeling of ion-exchange and solubility in low salinity water flooding. In *SPE Improved Oil Recovery Symposium*. Society of Petroleum Engineers.

Peng, J., Yi, H., Song, S., Zhan, W., & Zhao, Y. (2019). Driving force for the swelling of montmorillonite as affected by surface charge and exchangeable cations: A molecular dynamic study. *Results in Physics*, 12, 113-117.

Pouryousefy, E., Xie, Q., & Saeedi, A. (2016). Effect of multi-component ions exchange on low salinity EOR: Coupled geochemical simulation study. *Petroleum*, 2(3), 215-224.

Qiu, J., Li, G., Liu, D., Jiang, S., Wang, G., Chen, P., ... & Lyu, X. (2019). Effect of Layer Charge Density on Hydration Properties of Montmorillonite: Molecular Dynamics Simulation and Experimental Study. *International Journal of Molecular Sciences*, 20(16), 3997.

Rahromostaqim, M., & Sahimi, M. (2018). Molecular dynamics simulation of hydration and swelling of mixed-layer clays. *The Journal of Physical Chemistry C*, 122(26), 14631-14639.

Rivet, S. M. (2009). Coreflooding oil displacements with low salinity brine (Doctoral dissertation, University of Texas at Austin).

Sharma, M.M., Filoco, P.R., 1998. Effect of Brine Salinity and Crude-Oil Properties on Oil Recovery and Residual Saturations, SPE 65402, *SPE ATCE*. New Orleans.

Skipper, N. T., Sposito, G., & Chang, F. R. C. (1995). Monte Carlo simulation of interlayer molecular structure in swelling clay minerals. 2. Monolayer hydrates. *Clays and Clay minerals*, 43(3), 294-303.

Speight, J. G. The Chemistry and Technology of Petroleum 5th ed.; *CRC Press*: Boca Raton, FL, 2007.

Stucki, J. W., Low, P. F., Roth, C. B., & Golden, D. C. (1984). Effects of oxidation state of octahedral iron on clay swelling. *Clays and Clay Minerals*, 32(5), 357-362.

Sun, L., Tanskanen, J. T., Hirvi, J. T., Kasa, S., Schatz, T., & Pakkanen, T. A. (2015). Molecular dynamics study of montmorillonite crystalline swelling: Roles of interlayer cation species and water content. *Chemical Physics*, 455, 23-31.

Tang, G. Q., & Morrow, N. R. (1999). Influence of brine composition and fines migration on crude oil/brine/rock interactions and oil recovery. *Journal of Petroleum Science and Engineering*, 24(2-4), 99-111.

Teich-McGoldrick, S. L., Greathouse, J. A., Jove-Colon, C. F., & Cygan, R. T. (2015). Swelling properties of montmorillonite and beidellite clay minerals from molecular simulation: comparison of temperature, interlayer cation, and charge location effects. *The Journal of Physical Chemistry C*, 119(36), 20880-20891.

Thomas, M. M., Clouse, J. A., & Longo, J. M. (1993). Adsorption of organic compounds on carbonate minerals: 1. Model compounds and their influence on mineral wettability. *Chemical Geology*, 109(1-4), 201-213.

Underwood, T., Erastova, V., Cubillas, P., & Greenwell, H. C. (2015). Molecular dynamic simulations of montmorillonite–organic interactions under varying salinity: an insight into enhanced oil recovery. *The Journal of Physical Chemistry C*, 119(13), 7282-7294.

Webb, K.J., Black, C.J.J., Al-Jeel, H., 2004. Low Salinity Oil Recovery – Log-Inject-Log. Paper SPE 89379 presented at the *SPE/DOE 14th Symposium on Improved Oil Recovery*. Tulsa, 17–21 April.

Xu, X., Liu, X., Oh, M., & Park, J. (2018). Swelling Capacity and Hydraulic Conductivity of Polymer-Modified Bentonite under Saline Water Conditions. *Applied Sciences*, 8(7), 1025.

Yildiz, H. O., & Morrow, N. R. (1996). Effect of brine composition on recovery of Moutray crude oil by waterflooding. *Journal of Petroleum science and Engineering*, 14(3-4), 159-168.

Yuan, B., & Wood, D. A. (Eds.). (2018). *Formation damage during improved oil recovery: Fundamentals and applications*. Gulf Professional Publishing.

Zhang, Y., Morrow, N.R., 2006. Comparison of Secondary and Tertiary Recovery with Change in Injection Brine Composition for Crude Oil/Sandstone Combinations. Paper SPE 99757 presented at the *SPE/DOE Symposium on Oil Recovery*. Tulsa, April.

Zhang, Y., Xie, X., Morrow, N.R., 2007. Waterflood Performance by Injection of Brine with Different Salinity for Reservoir Cores. Paper SPE 109849 presented at the 2007 *SPE Annual Technical Conference and Exhibition*. Anaheim, 11–14 November.

Zhang, Z. Z., & Low, P. F. (1989). Relation between the heat of immersion and the initial water content of Li-, Na-, and K-montmorillonite. *Journal of Colloid and Interface Science*, 133(2), 461-472.

Appendix 1. Listing of system data

Table 6. The system parameter of the LSW layer

Width, Å	Length, Å	Height, Å	Volume, Liters	Density, g/cm3	Volume, cm3	Mass, g	Number of Atoms
20.67	35.8245	10.330	7.6519E-24	1	7.6519E-21	7.6519E-21	256

Table 7. System details of S1

Ion	Number of Atoms	Molar mass, g/mol	Mass, mg	Volume, Liters	Concentration, ppm	Concentration, mol/L
Na^+	9	23	7.64E-20	7.65194E-24	44921.875	1.953125001
Cl^-	2	35.5	1.18E-19	7.65194E-24	15407.986	0.434027778

Table 8. System details of S2

Ion	Number of Atoms	Molar mass, g/mol	Mass, mg	Volume, Liters	Concentration, ppm	Concentration, mol/L
Na^+	4	23	7.64E-20	7.65194E-24	19965.278	0.868055556
Cl^-	2	35.5	1.18E-19	7.65194E-24	14469.76	0.407599

Table 9. System details of S3

Ion	Number of Atoms	Molar mass, g/mol	Mass, mg	Volume, Liters	Concentration, ppm	Concentration, mol/L
Na+	2	23	7.64E-20	7.65194E-24	9982.639	0.434027778
Cl-	2	35.5	1.18E-19	7.65194E-24	15407.986	0.434027778

Appendix 2. Raw RDF profile between the sodium and hydrogen oxygen (Na-H)

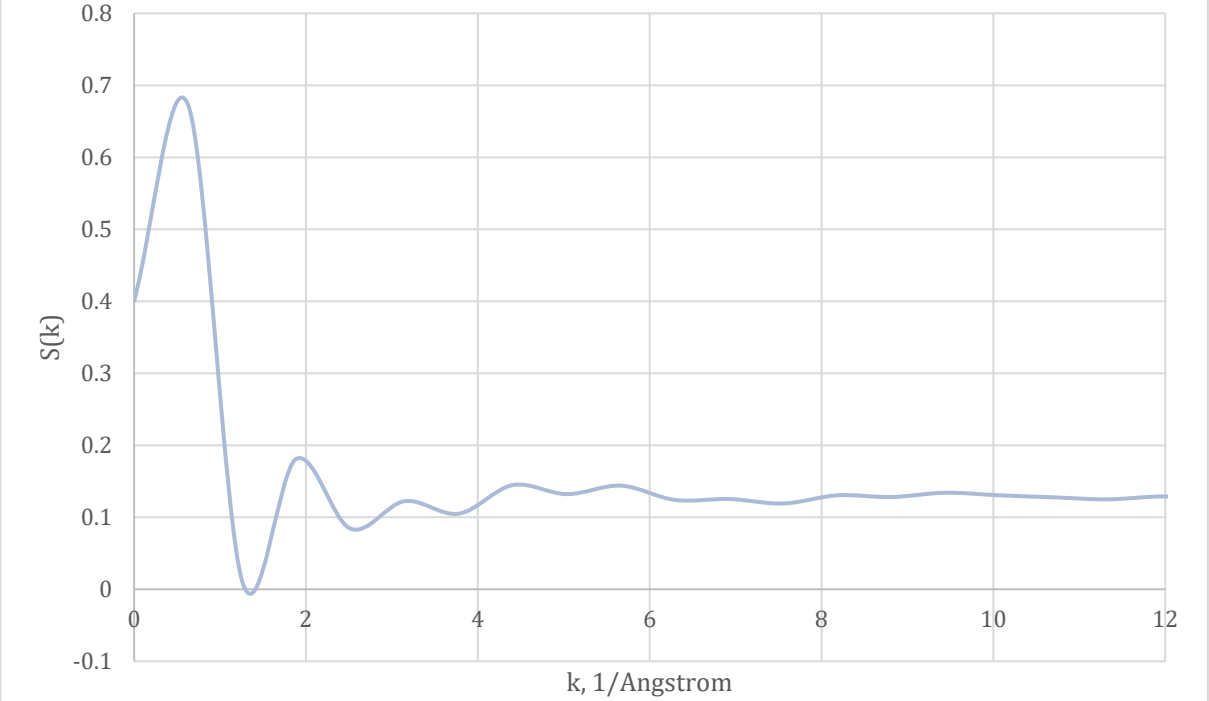

Figure 32. Structure factor between sodium and hydrogen oxygen for the system S1

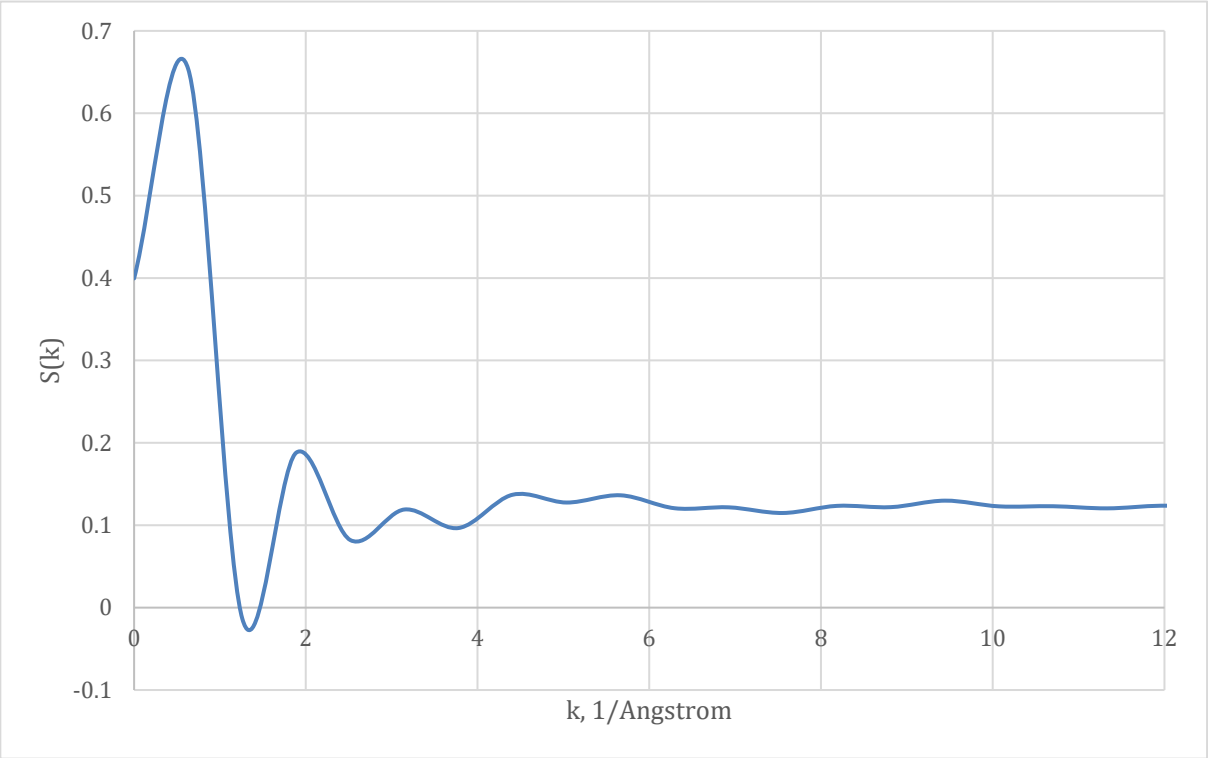

Figure 33. Structure factor between sodium and hydrogen oxygen for the system S2

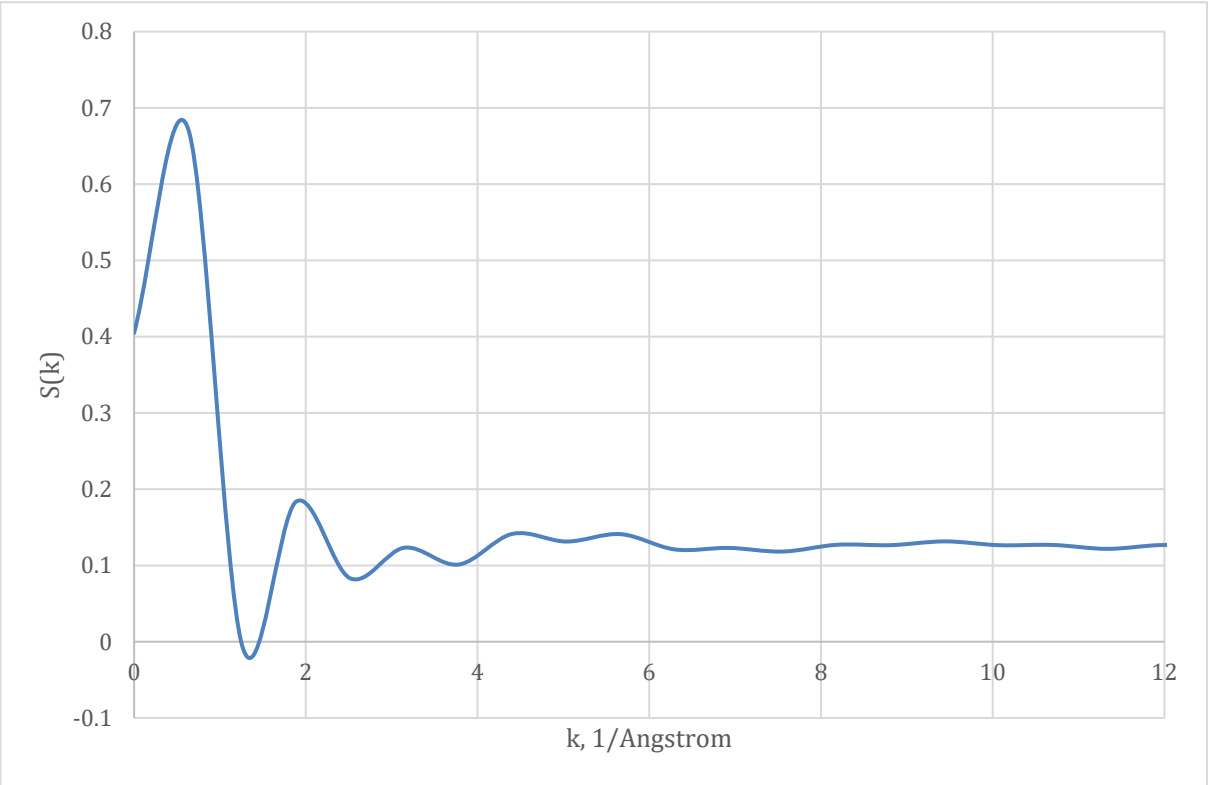

Figure 34. Structure factor between sodium and hydrogen oxygen for the system S3